Improvements to the Modeling of Average Floc Size in Turbulent Suspensions of Mud

Rachel Kuprenas

Thesis submitted to the Faculty of the

Virginia Polytechnic Institute and State University

in partial fulfillment of the requirements for the degree of

Master of Science

in

Civil Engineering

Kyle B. Strom, Chair

Nina Stark

Robert Weiss

May 7th, 2018

Blacksburg, Virginia

Keywords: Cohesive Sediment, Flocculation, Floc-size Modeling

Improvements to the Modeling of Average Floc Size in Turbulent Suspensions of Mud

Rachel Kuprenas

ABSTRACT

The accuracy of sediment transport models depends on identifying an appropriate sediment settling velocity. Determining this value for mud suspensions can be difficult because cohesive mud particles can aggregate, forming flocs whose sizes are a function of hydrodynamic and physiochemical conditions of the suspension. Here we present a new model refining the predicted floc size based on hydrodynamic conditions and inherited floc sizes, as well as on the salinity of the fluid environment. The improvements come from modifications made to the Winterwerp [1998] (W98) model. These improvements include: limiting floc size to the Kolmogorov microscale and including an initial salinity dependence. Limiting floc size in this way brings the model predictions more in line with flocculation theory and experimental observations. The salinity dependence was introduced based on a preliminary set of experiments that were conducted to examine floc growth rate and equilibrium size under different salinity conditions. In these experiments, change in salinity from 2.5 to 10 PSU did not affect equilibrium floc size. However, the increases in salinity did result in longer times to equilibrium and an apparent increase in floc density or fractal dimension. The modified W98 model allows calibrated aggregation and breakup coefficients obtained under one set of concentration values (for both sediment and salinity) to be used to predict floc size under other concentration conditions. Comparing the modified W98 model with laboratory data shows more accurate predictive values, indicating that the modified W98 equation is a promising tool for incorporation into larger sediment transport models.

This work was supported in part by ExxonMobil and the Virginia Sea Grant

Improvements to the Modeling of Average Floc Size in Turbulent Suspensions of Mud

Rachel Kuprenas

GENERAL AUDIENCE ABSTRACT

In order to assist in efforts to improve the environments of rivers, oceans, and estuaries, it is essential for scientists to have the ability to model all of the processes involved. One of the more difficult processes to model is sediment transport, specifically, cohesive sediment transport. How quickly a particle settles out of the water, and thus, how far a particle travels, is related to the density, size, and shape of the particle. With non-cohesive particles, this results in a relatively simple model as the particles stay the same size, shape, and density throughout time and space; however, cohesive particles are constantly changing as they can grow and shrink depending on the properties of the water at any given time. This process is called flocculation, and resulting particles are called flocs. This study aims to improve the modeling of cohesive sediment in the water column. Using existing data from [Tran et al., 2018], improvements were made to the existing Winterwerp [1998] model to account for the dependency of the particle size on sediment concentration. Tests were then run to collect data on how salinity impacts flocculation. This data was then used to further modify the Winterwerp [1998] model in order to account for salinity. These modifications resulted in predictions that better matched laboratory data, indicating that the modified Winterwerp [1998] equation is a promising tool for incorporation into larger sediment transport models.

Acknowledgments

I would like to thank my advisor Dr. Kyle Strom for his support through my numerous life plan and research changes. It was a process and I have learned so much. I would also like to thank my committee members Dr. Nina Stark and Dr. Robert Weiss for their understanding throughout my graduate studies. I could not have done with without you.

I owe many thanks to Adam Masters, Tank Sizemore, and my parents, Michael and Anne Kuprenas, for coming with me on numerous trips to the Chesapeake Bay. Stomping around in 40 degree water was much more fun when I had company. Also, my parents and grandparents (especially Bill Curry) have my undying appreciation for their assistance in editing.

Finally I would like to thank both ExxonMobile and the Virginia Sea Grant for their financial support throughout my studies.

Contents

List of Figures

List of Tables

Chapter 1

Introduction

1.1 Overview

Scientists and engineers rely on physics-based models to evaluate the transport and deposition of sediment in water systems. The accuracy of such models depends heavily on the selection of an appropriate sediment settling velocity, w_s [Dyer, 2014, Winterwerp, 2002, Geyer et al., 2004, Harris et al., 2005, Partheniades, 2009, Chen et al., 2010]. The terminal settling velocity of cohesive and non-cohesive sediment is determined by sediment size, density, and shape [Rubey, 1933, Dietrich, 1982, Strom and Keyvani, 2011]. For non-cohesive sediment, the settling velocity is relatively easy to calculate as the size, density, and shape of the particles are not changing. However, for cohesive particles, which can form flocs, the settling speed is not as simple. The reason for the added complexity is

that cohesive particles can create aggregates, called flocs, which are orders of magnitude larger than the primary constituent grain of the aggregate [Van Leussen, 1994] (Fig. 1.1). Furthermore, the flocs can grow or shrink in size depending on environmental conditions such as sediment mineralogy, water column chemistry and organic content, suspended sediment concentration, turbulent shear stress, and floc shape [Krone, 1963, Dyer, 2014, Winterwerp and van Kesteren, 2004, Partheniades, 2009, Tang et al., 2014, Guo et al., 2017]. In particular, sediment concentration, C [mass/vol], and mean turbulent shear rate, G, are often thought to be the key determiners of flocs size for a particular system with constant sediment type, biological content, and salinity. G is typically taken to be a quantitative measure of turbulent mixing:

$$G = \sqrt{\frac{\varepsilon}{\nu}} = \frac{\nu}{\eta} \tag{1.1}$$

where ν is the kinematic viscosity of the water, η is the Kolmogorov microscale, and ϵ is the dissipation rate of turbulent kinetic energy. The Kolmogorov microscale refers to the scale at which viscous effects are dominant.

In order to predict the hydrodymanics and sediment transport of a system, it is essential to create a model for a dynamic settling velocity that is reflective of the flocculation process. For both sediment concentration and water column chemistry (specifically salinity), there have been conflicting studies on how these parameters impact floc size. To create a versatile flocculation model, it is essential to determine how both concen-

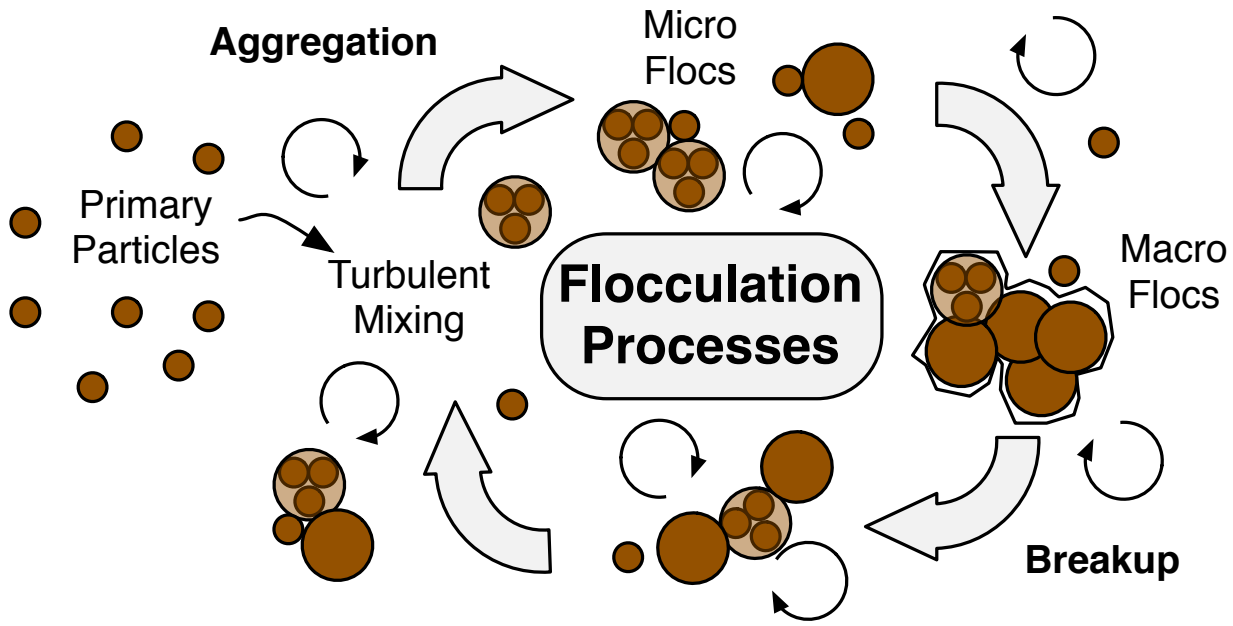

Figure 1.1: Flocculation process schematic

tration and salinity impact floc size as in most estuaries, these parameters change over time. It is necessary to model the floc size in order to predict accurate settling velocities of flocs. The settling velocity of flocs will be discussed in more detail in the Flocculation Modeling section

As discussed in the next section, the Winterwerp model can be used to describe the growth and breakup for flocs for fixed G, C, and S conditions using calibration parameters specific to those conditions. However, in dynamic conditions where these variables change, the calibration coefficients obtained at one set of values sometimes produce unrealistic model behavior. This study aims to improve the ability of the Winterwerp model to handle these changing conditions. To accomplish this, time series data is required to show how floc growth rates and equilibrium sizes (terms explained below) are related

to changes in C and S. The Previous and Related Work section given below summarizes the basic known influencers of flocculation and the literature pertaining to the role that suspended sediment concentration and salinity have on flocculation. Included in the section is also an overview of the way in which flocculation effects have been included in sediment transport modeling and a detailed description of the Winterwerp average floc size model. The specific study objectives and methods outline are then given at the end of this Introduction chapter.

1.2 Previous and Related Work

Flocculation is the process by which cohesive particles aggregate and breakup within the water column [Krone, 1962, Winterwerp and van Kesteren, 2004]. Cohesive particles (clay) aggregate when they are close enough together that the van der Waals attractive force is able to overcome the the net repulsive force of the particles [Partheniades, 2009]. It has been shown that there is a typical growth rate associated with flocs [Keyvani and Strom, 2014]. Droppo [2001] listed five attributes that impact floc behavior: inorganic content, biota and bioorganic content, water, and pores. These characteristic impact the floc in the following ways:

- The inorganic content can impact the floc density, bacterial colonization, and electrochemical effects (making it easier or harder to overcome the repulsive force of the particles).

- The bacterial colonization and bioorganic content impact the flocs' growth rate and equilibrium size, the electro-chemical effects, the density, and the nutrient/contaminant absorption.

- The water can impact the floc by changing the floc hydrodynamics, affecting the electro-chemical characteristics, and reducing the floc density.

- Finally, the pores of the floc can impact the floc characteristics by changing the floc hydrodynamics, reducing the floc density, and changing the bio-chemical gradients Droppo [2001].

All of these characteristics can influence the density of the floc. The varying density of the floc becomes important when modeling the deposition of the suspended sediment.

The deposition pattern of the suspended sediment is largely a function of the sediment settling velocity, w_s [Dyer, 2014, Geyer et al., 2004, Harris et al., 2005]; therefore, modeling the settling velocity of the sediment is vitally important in modeling the sediment transport. The settling velocity of sand is relatively simple as the w_s is a function of the size, density, and shape of the particles [Rubey, 1933, Ferguson and Church, 2004]. The settling velocity of cohesive sediment is largely a function of those same parameters; however, the size, density, and shape of the particles are constantly changing within the water column [Strom and Keyvani, 2011, Krone, 1963, Dyer, 2014]. For flocs, the settling velocity is a function of the primary particle size D_p, the floc size D, and the fractal dimension of the floc n_f. For flocs, n_f values are between 1.5 and 2.5, with an n_f of 3

denoting a perfect sphere [Strom and Keyvani, 2011]. The fractal dimension can have a dramatic effect on the area of the floc as a change in the fractal dimension from 2 to 3 causes a reduction in area by a factor of 10 [Bowers et al., 2017]. The shear rate of the water column can impact the fractal dimension of the floc [Stone and Krishnappan, 2003]. Stone and Krishnappan [2003] found a parabolic effect of shear. When going from low shear to medium shear, floc size decreased and fractal dimensions increased; however, at the highest shear rates flocs are more irregular in shapes and the fractal dimension decreases due to increased particle collisions [Stone and Krishnappan, 2003].

Flocs have been found to range in size from 50-5000 μm [Alldredge and Cotschalk, 1988, Fennessy et al., 1994, Syvitski et al., 1995, Sternberg et al., 1996, Diercks and Asper, 1997]; for these experiments, the primary particle size ranged from 4 to 12 μm. The variation in floc size is a result of the mineral and organic composition of the mud [Krone, 1963], the time history of the mixture to turbulent shear [Van Leussen, 1994], the chemical properties of the water [Xia et al., 2004], and the concentration of the suspended sediment [Krone, 1978, Manning and Dyer, 1999].

The mineral and organic composition can affect the sticking efficiency of the sediment, [Winterwerp and van Kesteren, 2004]. This sticking efficiency modifies the theoretical aggregation rate by accounting for the fact that not every collision results in flocculation. The sticking efficiency is influenced by the type of clay in suspension, and by the number and type of cations present in the water. If there is an increase in the cation exchange capacity or the number of cations in the water, the sticking efficiency

increases and the flocs grow faster [Logan, 1999, Partheniades, 2009].

A more thorough discussion of the impact of turbulent shearing, suspended sediment concentration, and salinity on floc size and density is give below.

1.2.1 Turbulent Shear

Turbulent shear is one of the largest influencers of flocculation in the water column. There are three main drivers of flocculation in the water column: Brownian motion, differential settling, and turbulent mixing [Burban et al., 1989, Eisma et al., 1991, Huang, 1994].

Brownian motion (or the random motion of particles) has been shown to be negligible in estuaries and coastal regions [McCave, 1984, Van Leussen, 1994]. Differential settling, which is flocculation due to different settling velocities of particles, has also been shown to be unlikely in marine environments [Stolzenback and Elimelich, 1994, Hill et al., 1998]. This is because flocs formed by differential settling have extremely low density and are therefore relatively easy to breakup. Differential settling could become important in low energy systems [Hill et al., 1998]; however, the typical turbulence scales in marine environments make it unlikely for differential settling to have a large effect [Krone, 1986].

Turbulent shear is widely accepted as the primary driver of the collisions needed to promote aggregation in marine environments and has been described by Parker

et al. [1972]. These authors related G, a dissipation parameter, to both aggregation and breakup of flocs (eq. 3.1).

The collisions caused by turbulent shear drive floc growth; however as the turbulent shear increases, the floc size decreases [Kumar et al., 2010, Oles, 1992]. This is due to the impact of the Kolmogorov microscale. The Kolmogorov microscale is the smallest eddy contained within the flow. If the floc is smaller than η (and thus, contained within a single eddy) then the floc experiences a shearing effect; however, if the floc is larger than η then the floc experiences eddies which cut through the floc [Parker et al., 1972]. This results in flocs which experience higher shear as the floc grows to η and results in an equilibrium floc size which is proportional to η [Tambo and Hozumi, 1979, Akers et al., 1987, van Leussen, 1988, Dyer, 2014, Kumar et al., 2010, Coufort et al., 2005, Braithwaite et al., 2012, Parker et al., 1972, Ramírez-Mendoza et al., 2016, Wiesner, 1992].

1.2.2 Concentration

The impact of sediment concentration on floc size varies between studies. There have been some studies that found that there is an increase in floc size with concentration [Gratiot and Manning, 2004, Oles, 1992, Eisma and Li, 1993, Tran et al., 2018], and others that say that floc size decreases or is unaffected by suspended sediment concentration. The Gratiot and Manning [2004] study looked at concentrations up to 8 g/l and found that at high concentrations, nearly all sediment was contained in flocs greater than 120

μm. This is interesting because for lower concentrations, the sediment tended to divide to a bimodal distribution of microflocs and macro flocs (where microflocs were flocs less than 120 μm and macroflocs were flocs which were greater than 120 μm). The Eisma and Li [1993] study looked at the Dollard Estuary and measured flocs in-situ. In the Dollard, during ebb tide, maximum floc size occurred during the maximum suspended matter concentration; however, the floc size continued to increase towards the high-water slack tide. This indicates that the flocs are not in equilibrium with the suspended matter at all times. Regardless, the flocs are likely formed during the time periods with high suspended matter concentration [Eisma and Li, 1993].

While several studies have shown that floc size increases with increasing suspended sediment concentration, there have also been studies that show there is no relation between concentration and floc size [Mikeš and Manning, 2010, Manning and Dyer, 1999, Milligan and Hill, 1998]. Mikeš and Manning [2010] included both laboratory studies as well as field surveys. Interestingly, for the laboratory studies, floc size was shown to increase with concentration, but when field surveys were conducted, there was no clear link between the floc size and concentration. Similar disparate results have been found for salinity and turbulence [Mikeš and Manning, 2010]. This seeming discrepancy could be due to several factors all changing with time, which makes it difficult to determine how floc size is related to an individual parameter. Manning and Dyer [1999] also found conflicting results when changing more than one parameter with an impact on flocculation. Manning and Dyer [1999] found that for low shears, high concentrations

produced the larger flocs; however, for high shears, high concentrations actually caused smaller flocs. Manning and Dyer [1999] suggested that this is due to more two and three body collisions caused by high shear and high concentration. While the previously mentioned studies found no clear link between concentration and floc size when multiple variables were looked at, Serra et al. [1996] found that below a certain threshold concentration (volume fraction equal to $2x10^{-5}$, or approximately 50 mg/L), floc size is almost independent of concentration and is only dependent on turbulent shear.

Floc size has also been found to decrease with concentration in some studies [Burban et al., 1989, Tsai et al., 1987]. Both Burban et al. [1989] and Tsai et al. [1987] conducted laboratory experiments with concentrations ranging from 10 mg/L to 800 mg/L using sediment collected from the Detroit River inlet to Lake Erie. While these studies found clear decrease in floc size with concentration, it is important to note that the composition of the sediment has a significant impact on equilibrium floc size [Milligan and Hill, 1998]. As the sediment used in these experiments was from a natural source, it is possible that the composition for each experiment was not exactly the same. Additionally, using this same argument, it is possible that for the specific make up of the sediment within the Detroit River inlet to Lake Erie, concentration does cause a decrease in floc size; however, this might not be universal for all sediment. Additionally, the decreasing floc size with concentration could be explained with the idea that while an increase in concentration does cause an increase in collisions, and thus, should increase aggregation, the higher concentrations also have a large number of three-body collisions which

can enhance disaggregation [Burban et al., 1989, Manning and Dyer, 1999].

In a companion study to the one presented in this thesis, Tran et al. [2018] conducted mixing tank experiments on sediment concentrations ranging from 50 mg/L to 400 mg/L. Tran et al. [2018] found that while concentration did increase floc size, it only increased floc size by 20% over a concentration increase of 800%.

1.2.3 Effect of Salinity

While flocculation has been observed in freshwater environments [Guo and He, 2011], the rate can generally be increased with the addition of salt [Burns et al., 1997, Tawari et al., 2001]. While Guo and He [2011] observed flocculation in freshwater environments, others have found that no flocculation occurs below a certain salinity. Henceforth, this salinity will be referred to as the critical salinity (S_c). Ariathurai [1974] found that the critical salinity level for aggregation was in the range of 0.6-2.4 PSU (practical salinity unit). This agrees with Krone [1963] which found that the critical salinity level was between 1 and 3 PSU. The studies discussed in the section used either PSU or parts per thousand (PPT) to report the salinity level. PSU is determined by measuring the conductivity, while PPT measures the mass-volume concentration. Measured comparisons between PPT and PSU have been found to differ by a maximum of only 0.02 PSU. Thus, for clarity and comparison, values from these studies will be reported in PSU.

For the majority of clay particles, the addition of salt increases the flocculation rate.

The theory that is used to explain this behavior is the the DVLO theory [Verwey and Overbeek, 1948] and Derjaguin and Landau [1941]. In general, individual clay particles have a surrounding boundary layer that is negatively charged. This causes particles to repel each other as they get closer together. When positive ions (salts) are added to the water, the ions will attach to the negatively charged particle. This will neutralize the charges on the particles, and allow the particles to aggregate [Logan, 2012]. SenGupta and Papadopoulos [1998] looked specifically at the energy barrier preventing particle aggregation and found that the addition of salt allowed particles to aggregate more easily. A study in the Ems estuary found that settling velocities increased as salinity increased [van Leussen, 1999]. Mietta [2010] found that the addition of salt both increased the equilibrium floc size, as well as decreased the time needed to reach equilibrium. The opposite effect (in which increasing salinity decreases the equilibrium floc size) has also been observed [Burban et al., 1989]. While the Burban et al. [1989] study did find a decrease in floc size when comparing salt water flocs to fresh water flocs, the study also found that the salt water flocs reached equilibrium at a faster rate. Finally, there have been a few studies that have found no correlation between salinity and floc properties [Burt, 1986, Chen and Eisma, 1995, Eisma et al., 1991]. Burt [1986] attributed the differences in the results to the difference in in-situ field data and experimental data; however the difference in observations could be explained by the range of salinities being tested, as there seems to be a greater change when increasing the salinity from 0 to 10 PSU, while there is almost no difference in floc size when the salinity is increased from 10

to 35 PSU [Krone, 1963]. The difference in effect when considering higher and lower salinity levels is discussed below

In a study by Portela et al. [2013], sediment was placed in a stagnant settling column with different levels of salinity after experiencing turbulence; it was found that settling velocities increase by a factor of 6.5 between freshwater and marine conditions. This study also found that after five hours, 45% of sediment was still in suspension for freshwater, while only 10% for salinities between 10 and 30 PSU. An additional finding of this study was that an increase in salinity had little effect on the settling velocity after a salinity of 10 PSU. Krone [1963] also found a limit to the effect of salinity. Krone [1963] found that there was no significant change in the settling velocity of the sediment once the salinity was above 5 PSU. While most of these studies found that the limit on the effect of salinity was at or below 10 PSU, Owen [1970], using settling velocities, found that the limit occurred between 28 and 43 PSU depending on the sediment concentration. The Owen [1970] study also found that above that limit, salinity actually caused a decrease in settling velocity. This was attributed to salinity changing the density of the flocs rather than a decrease in floc size. Migniot [1968] also found that low concentrations and high concentrations were affected differently by an increase in salinity. In the Migniot [1968] study, for low concentrations, the limit for which salinity effected floc size was 3 PSU; however, for high concentrations, the limit was 10 PSU. A summary of these findings can be found in table 1.1.

When looking at floc characteristics other than size, Al Ani et al. [1991] found that

Study	Clay Type	Method	Finding
Ariathurai [1974]	Kaolinite	Theoretical	S_c = 0.6 g/L
	Illite		S_c = 1.1 g/L
	Montmorillonite		S_c =2.4 g/L
SenGupta and Papadopoulos [1998]	N/A	Theoretical	Floc size increases
van Leussen [1999]	Field	Settling	Floc size increases
Mietta [2010]	Kaolinite	Mixing Jar+Lazer diffusion	Floc size increases
Eisma et al. [1991]	Field	in-situ	No effect
Burt [1986]	Field	Settling	No effect
Chen and Eisma [1995]	Field	Settling	No effect
Burban et al. [1989]	Field	Couette+particle size analyzer	Decreases floc size
Portela et al. [2013]	Field	Settling	Limit
Krone [1962]	Field	Settling	Limit
Owen [1971]	Field	Settling	Limit
Migniot [1968]	Kaolinite	Settling	Limit

Table 1.1: Previous studies on the effect of increasing salinity on floc size

for a floc size of 500 μm, the density of the floc increases as the salinity is increased from 0-15 PSU and then hits a maximum at 10-15 PSU. At higher salinities flocs decreases in density at a similar rate to the initial increase. If flocs are taken to be 3D fractal structures, then an increase in density would be tied to an increase in fractal dimension [Kranenburg, 1994]. As with the impact of salinity on floc size, there have a been a few conflicting studies on the impact of salinity on fractal dimension. Using basic boundary layer theory, an increase in salinity should cause a decrease in fractal dimension as the

particles move from a reaction limited state (in which particles have a large repulsive force to overcome), to a diffusive limited state (in which particles are only limited in growth by how often collisions occur [Logan, 2012]). Nonetheless, Waite et al. [2001], using aluminum oxide particles, also found that fractal dimension increased as salinity increased; however, there have been studies that have shown the opposite. Tawari et al. [2001] studied kaolnite clay, and using a sample cell and a light scattering technique, found that an increase in salinity caused a decrease in fractal dimension. While not measuring the fractal dimension directly, if one uses a flocculation model, such as the Winterwerp [1998] model, an increase in n_f causes an increase in time to equilibrium. A more thorough description of the Winterwerp [1998] model can be found in section 1.5.1. Therefore results from both Burns et al. [1997] and Mietta [2010], in which an increase in salinity was found to decrease the time to equilibrium, could indicate that an increase in salinity decreases the fractal dimension. A final aspect of impact of salinity on floc properties can be found in a study by Eisma et al. [1991]. Using in situ field sediment and pipettes, floc strength was found to decrease with increasing salinity. A summary of these studies can be found in table 1.2.

Salinity has also not been implemented into any physics-based flocculation models (though it has been included in some models that work off of local conditions). Because of the conflicting data, this study aims to better quantify and determine the impact of salinity on floc size.

Study	Clay Type	Method	Finding
Al Ani et al. [1991]	Field	Settling	Parabolic effect on floc density
Waite et al. [2001]	Aluminum Oxide	Sample cell+light scattering	Increases n_f
Tawari et al. [2001]	Kaolnite	Sample cell+light scattering	Decreases n_f
Burns et al. [1997]	Latex	Sample cell+light scattering	Decreases time to equilibrium
Mietta [2010]	Kaolinite	Mixing Jar+Laser diffusion	Decreases time to equilibrium
Eisma et al. [1991]	Field	in-situ+pipette	Floc strength decreases
Lee et al. [2002]	Field+model	Settling	With high G: increases n_f. With low G: decreases n_f

Table 1.2: Previous studies on the effect of increasing salinity on floc characteristics

1.2.4 Flocculation Modeling

Single Characteristic Floc Size

Modeling of flocculation has been done several different ways. One of the most common ways of modeling flocculation is by modeling a single characteristic floc size. The modeling of a characteristic floc size allows for a flocculation model to easily be implemented into a larger sediment transport model. Modeling flocculation using a single characteristic floc size has been done by Winterwerp [1998] and Maerz and Wirtz [2009]. The Winterwerp [1998] will be discussed in detail as this model is used as a base for the modified model developed in this study. Henceforth, this model will be referred to as

the W98 model.

In this section the key components of the W98 model are described. This description includes: an outline of the time-dependent model (section: Model basics) and a discussion on the basis for choosing particular model coefficients and the model functionality (section: Model parameters and time dependent functionality).

Model basics

The W98 model can be written in either an Eulerian or Lagrangian frame of reference. For the sake of simplicity we will discuss the original Lagrangian formulation. In this frame, a basic conservation equation for floc number density, n (number of particles or flocs per volume of mixture) can be expressed as:

$$\frac{dn}{dt} = \left(\frac{dn}{dt}\right)_{break} - \left(\frac{dn}{dt}\right)_{agg} \tag{1.2}$$

Here the floc aggregation and breakup kernels, on the righthand side of the equation, are in terms of the rate of change of the particle number density due to either aggregation or breakup respectively. These terms will be discussed in detail below. In this formulation, particles cannot be gained or lost through anything other than aggregation and breakup (e.g., deposition). Also note that aggregation results in a decrease in the number density and that breakup leads to an increase in n.

The floc number density, n, is related to the mass concentration, C, and floc prop-

erties of size and composition as follows:

$$n = \frac{C}{f_s \rho_s} D_p^{n_f - 3} D^{-n_f} \tag{1.3}$$

where D_p is the size of the primary particles (or smallest constituent grains), D is the average floc size, n_f is the floc fractal dimension, and f_s is a shape factor, equal to $\pi/6$ for spherical particles or flocs. Equation 1.3 is based on a three-dimensional fractal structure of primary particles within the floc that allows for the floc size, D, to be related to the total number of primary particles in a floc, N_p (of size D_p) through the fractal dimension, n_f [Kranenburg, 1994]:

$$D = D_p N_p^{1/n_f} \tag{1.4}$$

Use of Equation 1.4 in turn allows for the floc submerged specific gravity, $R_f = (\rho_f - \rho)/\rho$, where ρ_f is the floc density and ρ is the water density, to be expressed as a function of floc size, the size of the primary particles, and the fractal dimension of the flocs [Jiang and Logan, 1991, Kranenburg, 1994]:

$$R_f = R_s \left(\frac{D}{D_p} \right)^{n_f - 3} \tag{1.5}$$

where R_s is the submerged specific gravity of the primary particles. For a spherical particle, $n_f = 3$ and there is no difference between R_f and R_s. However, for flocs, n_f is always less than 3. This means that R_f will decrease with floc size following a negative power-law trend. The smaller the fractal dimension, the more loosely packed

and irregularly shaped the flocs will be and the more rapidly R_f will decrease with size. n_f is therefore a useful index for quantifying the packing arrangement of particles within flocs.

The aggregation kernel used in the W98 model is the Levich [1962] coagulation equation that gives the rate of decrease in the number density, n, due to shear-driven collisions and resulting aggregation:

$$\left(\frac{dn}{dt}\right)_{agg} = \frac{3}{2} e_c \pi e_d G D^3 n^2 \tag{1.6}$$

In Equation 1.6, e_d is diffusion efficiency and e_c is an efficiency parameter which accounts for the portion of collisions that result in flocculation. The parameter e_c is a function of the physico-chemical properties of the sediment and water.

For the breakup kernel, Winterwerp [1998] proposed that the rate change in n was a function of the relative size of the floc and the ratio of an applied stress on the floc and the strength of the floc:

$$\left(\frac{dn}{dt}\right)_{break} = anG \left(\frac{D - D_p}{D_p}\right)^p \left(\frac{\tau_t}{\tau_y}\right)^q \tag{1.7}$$

In this formulation, a, p, and q are coefficients that need to be determined, τ_t is the turbulent induced stress on the floc, and τ_y is the strength of the floc. Winterwerp [1998] reasoned that for flocs equal to or smaller than the Kolmogorov microscale, $D \leq \eta$, that

$\tau_t = \mu G$, and that the critical strength of the floc can be modeled as, $\tau_y = F_y/D^2$. In these two models, μ is the dynamic viscosity of the fluid and F_y is the floc yield strength in dimensions of force.

The primary conservation equation (Eq. 1.2) and the aggregation and breakup kernels (Eqs. 1.6 and 1.7) can be transformed to equations for rate of change in floc size by noting that,

$$\frac{dn}{dt} = \frac{dn}{dD}\frac{dD}{dt} \tag{1.8}$$

Taking the derivative of Equation 1.3 with respect to floc size, yields the change in number density with respect to floc size given the particular fractal structure of the floc:

$$\frac{dn}{dD} = -\frac{n_f C}{f_s \rho_s} D_p^{n_f-3} D^{-n_f-1} \tag{1.9}$$

Applying the chain rule transformation to equations 1.2, 1.6, and 1.7 and using the definition of dn/dD (Eq. 1.9) yields the Lagrangian form of the W98 model for dynamic floc size:

$$\frac{dD}{dt} = \frac{k_A^{'}}{n_f}\frac{{D_p}^{n_f-3}}{\rho_s} GCD^{4-n_f} - \frac{k_B^{'}}{n_f} DG\left(\frac{D-D_p}{D_p}\right)^p \left(\frac{\mu G}{F_y/D^2}\right)^q \tag{1.10}$$

Here $k_A^{'}$ is a dimensionless aggregation coefficient that is a function of the efficiency of statistical collisions to produce aggregation and the shape factor of the floc, i.e., $k_A^{'} = 3e_c \pi e_d/(2f_s)$; $k_B^{'}$ is a dimensionless breakup efficiency parameter previously called a in Equation 1.7, i.e., $k_B^{'} = a$. Both $k_A^{'}$ and $k_B^{'}$ are suspension-dependent calibration

parameters that are a net outcome of the sticking property of the sediment, which is influenced by primary particle size, sediment mineralogy, water chemistry, organic matter, and particle shape. Put in terms of dD/dt, the aggregation kernel, A, is:

$$A = \frac{k_A^{'}}{n_f} \frac{{D_p}^{n_f-3}}{\rho_s} GCD^{4-n_f} \tag{1.11}$$

and the breakup kernel, B, is:

$$B = \frac{k_B^{'}}{n_f} DG \left(\frac{D - D_p}{D_p} \right)^p \left(\frac{\mu G}{F_y/D^2} \right)^q \tag{1.12}$$

Model parameters and time dependent functionality

Solution of Equation 1.10 yields D as a function of time. This time varying, and/or space varying if using an Eulerian frame, D can then be used with a settling velocity equation to model floc settling velocities, w_s, that change with alterations in the driving conditions (primarily C and G). For examples see Winterwerp [1998] and Strom and Keyvani [2016]; in these cases $w_s = w_s(D, D_p, n_f, \rho, \rho_s, \nu)$ [Strom and Keyvani, 2011].

To solve the W98 equation (Eq. 1.10), one needs to define D_p, D_0, n_f, p, q, and F_y. Winterwerp [1998], and most subsequent studies that use Equation 1.10, take the fractal dimension of the mud flocs, n_f, to be 2 (though n_f is known to range between 1.8 and 2.5). When $n_f = 2$, p takes on a value of 1 ($p = 3 - n_f$). In all known uses of the W98 model, q has been set to 0.5. Son and Hsu [2008] confirmed that $p = 1$ and $q = 0.5$

are reasonable values to use from an equation stability perspective even when a variable fractional dimension model is used for n_f. Based on data from Van Leussen [1994], Winterwerp [1998] suggested a reasonable value of F_y for estuarine flocs is F_y = 1E-10 N. This value has again proven to be reasonable and is often used when modeling flocs with the W98 model [e.g., Son and Hsu, 2008, Keyvani and Strom, 2014, Strom and Keyvani, 2016], though Son and Hsu [2009] suggest that even better results can be obtained by letting F_y vary with floc size and fractal dimension.

Figure 1.2 shows the behavior of the solution under independent changes in G, C, n_f, k'_A, k'_B, and D_p away from a baseline condition. A change in F_y is not shown to limit the number of figures, but an increase in F_y generates the same trends in the model solution as a decrease in $k_B^{'}$. The initial condition for all solutions in the figure is $D(t = 0) = D_0 = D_p$, and the baseline conditions used to explore the functionality are: $G = 35$ s^{-1}, $C = 50$ mg/L, $D_p = 5$ μm, $n_f = 2$, $k_A^{'} = 1.17$, $k_B^{'} = 1.16$E-5, and F_y = 1E-10 N. In general, the basic form of the W98 model does a good job of capturing the trends in time for both aggregation and breakup [e.g., Strom and Keyvani, 2016].

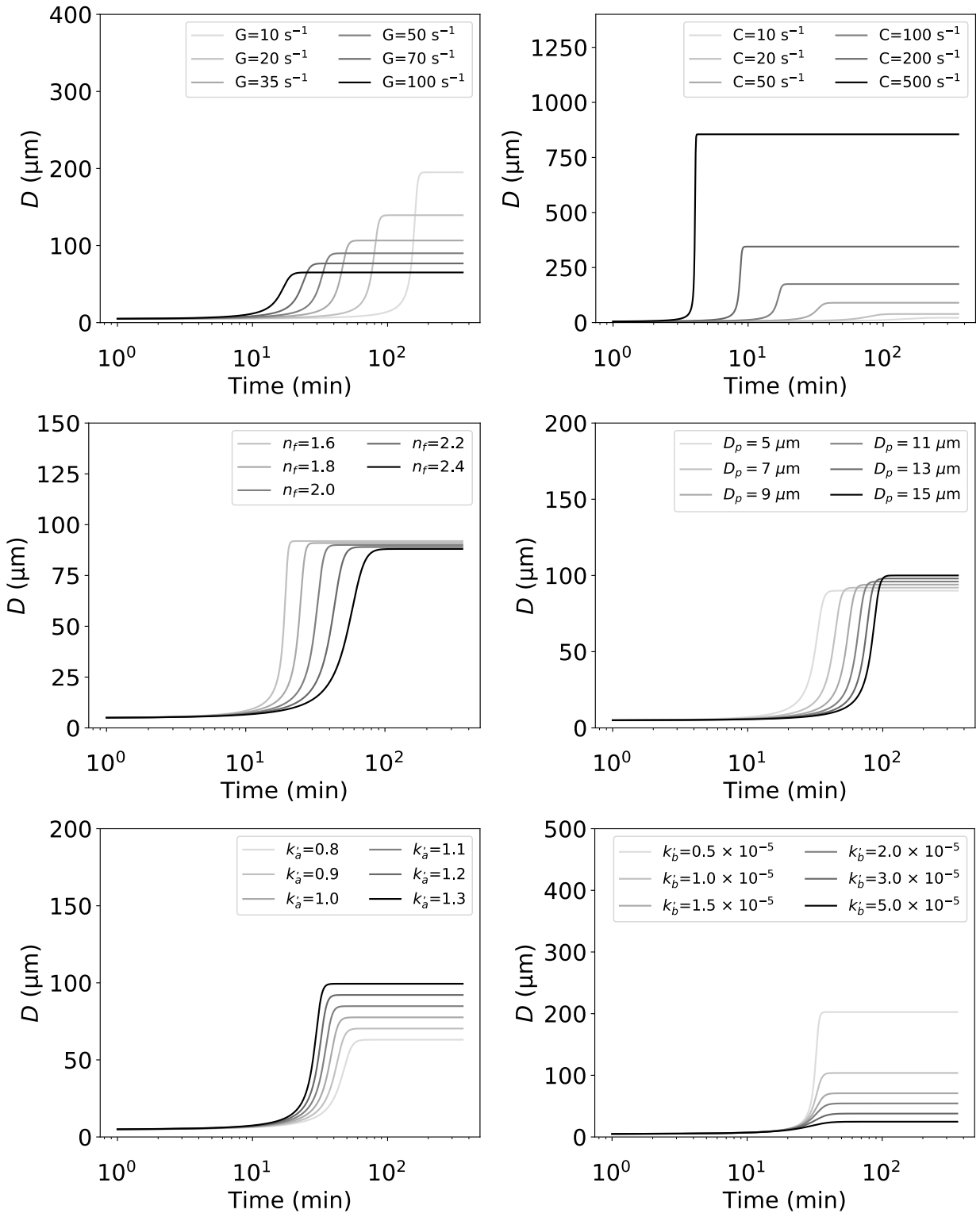

Figure 1.2: Functionality of Eq. 1.10. D is the floc size. The baseline conditions used to develop the figure are: $G = 35$ s^{-1}, $C = 50$ mg/L, $n_f = 2$, $k_A^{'} = 0.1$, $k_B^{'} = 1.5$E-6, and $F_y = 1$E-10 N with $D_p = 5$ μm.

If values for n_f, p, q, and F_y can be defined, then k_A' and k_B' (aggregation and breakup efficiency) are the only remaining parameters that must be defined to use the W98 model in a predictive way. Because these two parameters account for sediment and water specific properties that relate to the sticking properties of the mud suspension (such as clay type, ion type and concentration, and organic matter), it seems best to leave these parameters as general calibration parameters to be determined from experimental floc growth data such as in the studies of Winterwerp [1998] and Son and Hsu [2008]. Given a single set of conditions such as the growth of flocs from a primary-particle state in conditions of constant G, C, and water chemistry, reasonable values for k_A' and k_B' can be obtained. The model might not match the data particularly well in the transition from the fast growing state to the equilibrium state [Son and Hsu, 2008, 2009, Keyvani and Strom, 2014, Sherwood et al., 2017]; to better match the data in this region, one would either need to increase the fractal dimension with floc size or make k_A' and k_B' a function of floc size [Keyvani, 2013]. While values of k_A' and k_B' can be defined to reasonably capture the equilibrium size and the time to equilibrium, it has been shown or suggested that such k_A' and k_B' values might turn out to be functions of G or C [e.g., Son and Hsu, 2008, Keyvani and Strom, 2014, Strom and Keyvani, 2016]. Obviously, such behavior is not ideal as one would expect G and C to vary in coastal zones. What would be preferred is if the W98 model could be calibrated to a single floc growth experiment to obtain k_A' and k_B' and then used to predict changes in floc size outside of the range of conditions for which it was calibrated.

While the Winterwerp [1998] approach to single floc size modeling is more common, the single floc size can also be measured by using a distribution-based method [Maerz and Wirtz, 2009]. The Maerz et al. [2011] method is based on the continuous exponential floc number distribution rather than single size approach that Winterwerp [1998] uses. This method is similar to the theory used for full size-class population floc modeling.

Bimodal Approach

One of the less common approaches to flocculation is a bimodal approach, two-class size approach. This method uses the dense, smaller microflocs as one of the size classes, and the less dense, larger macroflocs as the other size class [Lee et al., 2011]. As stated previously, macroflocs tend to be flocs with a size of over 120 μm while microflocs are flocs with a size less that 120 μm [Gratiot and Manning, 2004]. The method used by Lee et al. [2011] uses three coupled equations which model the time rate of change of the number concentration of microflocs, the number concentration of macroflocs, and the number concentration of micro flocs bound in macroflocs.

$$\begin{aligned} \frac{dN_p}{dt} - \frac{\partial}{\partial z}\left(D_{tz}\frac{\partial N_p}{\partial z}\right) &= (A_p + B_p) - \frac{\partial(w_{s,p}N_p)}{\partial z} \\ (\mathrm{A}_p + B_p) &= -\tfrac{1}{2}\alpha\beta_{pp}N_pN_p\left(\tfrac{N_c}{N_c-1}\right) - \alpha\beta_{pp}N_pN_f + fN_caN_f \end{aligned} \tag{1.13}$$

$$\frac{dN_f}{dt} - \frac{\partial}{\partial z}\left(D_{tz}\frac{\partial N_f}{\partial z}\right) = (A_f + B_f) - \frac{\partial(w_{s,f}N_f)}{\partial z}$$
$$(\mathrm{A}_f + B_f) = \tfrac{1}{2}\alpha\beta_{pp}N_pN_p\left(\tfrac{1}{N_c-1}\right) - \alpha\beta_{pp}N_fN_f + fN_caN_f \tag{1.14}$$

$$\frac{dN_T}{dt} - \frac{\partial}{\partial z}\left(D_{tz}\frac{\partial N_t}{\partial z}\right) = (A_t + B_t) - \frac{\partial(w_{s,t}N_t)}{\partial z}$$
$$(\mathrm{A}_T + B_T) = \tfrac{1}{2}\alpha\beta_{pp}N_pN_p\left(\tfrac{1}{N_c-1}\right) - \alpha\beta_{pp}N_pN_f + FN_caN_f \tag{1.15}$$

Where the subscripts p, f, and T represent microflocs, macroflocs, and microflocs within macroflocs respectively, F is the fraction of microflocs created by the breakage of macroflocs ($1 - F$ is the fraction of smaller macroflocs created by larger macroflocs), α is the collision efficiency, β is the collision frequency, a is the breakage kinetic constant, N is is the number concentration, D is the floc size, and $w_{s,t}$ (settling velocity of microflocs within the macrofloc) is equal to $w_{s,f}$ (settling velocity of the macrofloc).

The bimodal model is beneficial in that it does manage to capture the microflocs and macroflocs which are found in nature without using the computational power that a full size-class model would need [Biggs, 1970, Li et al., 2017]; however, it is still more computationally expensive than a single size-class model. Therefore, it is still desirable to develop an accurate single size-class model for larger transport models.

Full Size-Class Approaches

Full size-class based approaches model the changes in floc size population [Lick and Lick, 1988, Burban et al., 1989, Hill and Nowell, 1995, McAnally and Mehta, 2000a, Ver-

ney et al., 2011]. These approaches still use the principle of mass conservation; however, the computations are much more complex. These approaches track the exchange between various size classes. The equations for each class size are similar to the single class-size methods in that there is a breakup and aggregation term for each class-size. The difference is that the different class-sizes interact with each other and thus, the approach allows for particle-particle collisions.

As with the single size-class models, the majority of these models have to be calibrated experimentally, which makes them difficult to implement on a broader scale. McAnally and Mehta [2000a] attempted to solve this difficulty by developing relationships between the clay and water chemistry properties for the various efficiency parameters; however, the relationships developed in that study have not been widely tested. Additionally, full size class approaches tend to be more computationally expensive, and thus, are not ideal for implementing into a larger sediment transport model. Sherwood et al. [2017] found that including flocculation in a sediment transport model increased the computational time by a factor of 60.

Finding Settling Velocity from Floc Size

Deriving an equation for the settling velocity of flocs is based on the same principles. Settling velocity equations for flocs are based on a balance between the fluid drag and weight, just as they are for solid particles; however, instead of using a constant density for the sediment, the density is allowed to change with the size of the floc. The following

equation expresses the balance between drag and weight:

$$w_s = \left(\frac{2VgR_f}{C_d A} \right)^{1/2} \tag{1.16}$$

In equation 1.18, V is the volume, g is the gravitational acceleration, R_f is submerged specific gravity of the floc, $R_f = (\rho_f - \rho_w)/\rho_w$, where ρ_f and ρ_w are the densities of the floc and water respectively, A is the area of the floc normal to the direction of motion, and C_d is the drag coefficient. R_f can be found using the equation 1.5 [Jiang and Logan, 1996, Kranenburg, 1994].

One common expression for the drag coeffecient which is used in several studies is [Winterwerp, 1998, Manning and Dyer, 1999, Khelifa and Hill, 2006]:

$$C_d = \frac{24}{Re}(1 + 0.15Re^{.687}) \tag{1.17}$$

where $Re = w_s d_f/\nu$ is the particle Reynolds number and ν is the viscosity of water. Another option for defining a mud settling velocity based on floc size is the explicit settling velocity equation of Strom and Keyvani [2011]:

$$w_s = \frac{gR_s D^{n_f - 1}}{b_1 \nu D_p^{n_f - 3} + b_2 \sqrt{gR_s D^{n_f} D_p^{n_f - 3}}} \tag{1.18}$$

where b_1 and b_2 are shape factors dependent on sediment shape and porosity. The suggested values for b_1 and b_2 for a fractal dimension of $n_f = 2$ are $b_1 = 20$ and $b_2 =$

1.258 [Strom and Keyvani, 2011].

While settling velocities have been shown to vary from 0.1 to 10 mm/s, Hill et al. [1998] found that the average value for settling velocity was 1 mm/s. Because of this, most larger transport models use a constant settling velocity of 1 mm/s [Geyer et al., 2004]. This does not take into account the flocs changing in size and density over time. In order to take these changes into account, some larger transport models use a different constant settling velocity for storm or non-storm events [EPA, 2010], allowing for a difference in sediment makeup depending on the hydrological conditions; however, this still does not take into account flocs changing in size or density over a period of time.

1.3 Study Objectives

Flocculation has been modeled in many different ways, with some models being more accurate or computationally faster than others. In this study, I focus on improving the average floc size model of Winterwerp 1998. The model is simple and captures many of the basic trends in floc growth and breakup, but it has been shown that the model can predict unrealistic floc sizes when used in concentration conditions outside of those for which the model was calibrated. Additionally, no method currently exists within the formulation to account for changes in water column chemistry (such as the addition or loss of salt ions). Therefore, the objectives of my study are to:

1. improve the behavior of the W98 model across a spectrum of suspended sediment concentration values; and

2. introduce to the model a dependence on salinity.

1.3.1 Approach

Time series data on floc growth in suspensions with different levels of concentration and salinity are needed to help develop and test modifications to the W98 model. Data for the first objective comes from the companion study of Tran et al. [2018]. Preliminary data needed to meet the second objective was developed as part of my study. The experiments were conducted in a laboratory mixing tank with salinities ranging from 0 to 10 PSU, and time series of floc growth were obtained with the floc imaging system of Tran et al. [2018].

The thesis document is organized around my two objectives. Chapter 2 presents the body of work aimed at addressing the first objective (modifying the W98 model to produce more reasonable values of floc size across a spectrum of concentration conditions). This component of the study has been submitted for publication. Chapter 3 discusses the portion of the study aimed at addressing objective two (incorporating salinity impacts in the W98 model).

The working premise of my study is that incorporating simple modifications, based on known process understanding, will allow calibration parameters for the Winterwerp

1998 model obtained from a specific set of conditions to be used more generally in conditions other than those for which they were calibrated. Specifically, I hypothesize that the study objectives can be met through model modifications that: (1) ensure floc size is limited, approximately, by the Kolmogorov microscale; and (2) make the aggregation coefficient a function of salinity.

Chapter 2

A shear-limited flocculation model for dynamically predicting average floc size

This chapter will examine the relationship between sediment concentration and floc size. Experimental data collected by Tran et al. [2018] will be used to modify the W98 to more accurately predict average floc size.

2.1 The need to re-calibrate the model for different values of C

We highlight the need to calibrate $k_A^{'}$ and $k_B^{'}$ in the original W98 formulation to particular conditions by exploring the model's behavior using the data of Tran et al. [2018]. The

study of Tran et al. [2018] examines the influence of suspended sediment concentration alone on the magnitude of the equilibrium floc size and the rate of change towards and equilibrium floc size in a turbulent suspension. This dataset will be discussed in more detail later on. For now, it is sufficient to introduce one set of experiments from this study, i.e., the Set A experiments. The experiments of interest examined the growth of flocs in a suspension from a primary-particle state up to an equilibrium floc size under constant turbulent shearing. The experiment was repeated multiple times for a variety of initial suspension concentrations ranging from 15 to 400 mg/L. The measured growth trends matched the general shape produced by solving the W98 model (Fig. 1.2), and as such, $k_A^{'}$ and $k_B^{'}$ values could be found for each experimental condition. Ideally, one would hope that calibration values for $k_A^{'}$ and $k_B^{'}$ found at one particular concentration could be used in a predictive way to describe the floc time series data for a different concentration. However, no individual pair of $k_A^{'}$ and $k_B^{'}$ values could be used to describe the time development of the flocs across all concentrations. For instance, Figure 2.1 shows a case where the $k_A^{'}$ and $k_B^{'}$ values obtained through calibration to the average floc size time series at $C = 50$ mg/L are used to predict the change in average floc size with time at $C = 400$ mg/L. The results are not that encouraging as the equilibrium values predicted by the model (using the coefficients calibrated for $C = 50$ mg/L) drastically over-predict the equilibrium floc size at $C = 400$ mg/L. For example, D_e of the model at $C = 400$ mg/L is 685 μm whereas the experiments show that D_e for this concentration and shear rate is $D_e = 132$ μm. To make the W98 model fit the data,

the ratio of $k_A^{'}/k_B^{'}$ has to be adjusted down for each increase in concentration (Eq. 2.4). The functionality of this decrease in $k_A^{'}/k_B^{'}$ is shown in Figure 2.2.

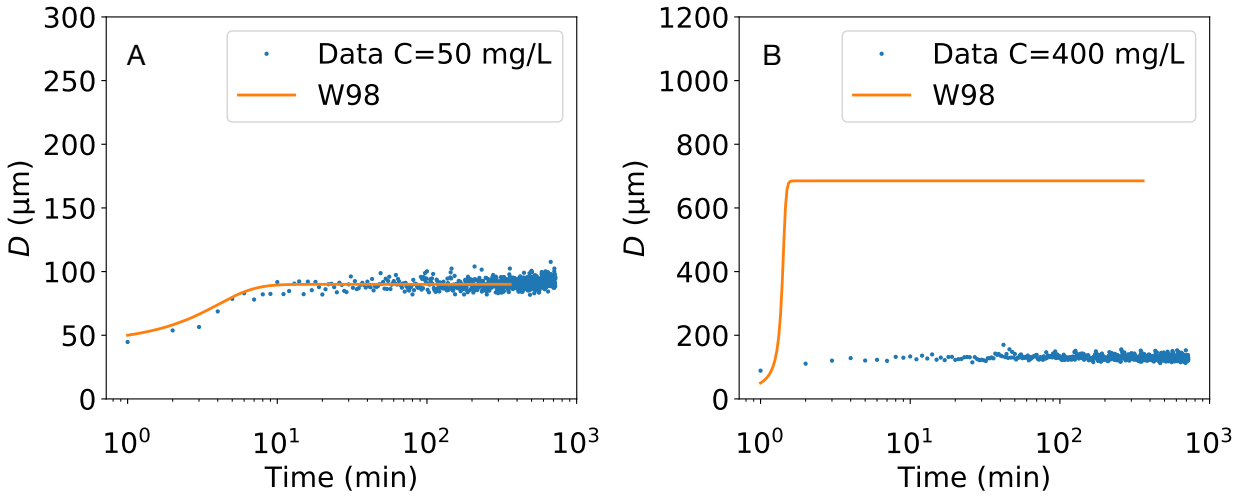

Figure 2.1: The W98 model compared with data from Tran et al. [2018] at (A) $C = 50$ mg/L, and (B) $C = 400$ mg/L. Here $k_A^{'}$ and $k_B^{'}$ values were first calibrated using the time series data from the experiment conducted at $C = 50$ mg/L (panel A). These $k_A^{'}$ and $k_B^{'}$ values were then used to predict the floc size time series at $C = 400$ mg/L using the W98 model (panel B).

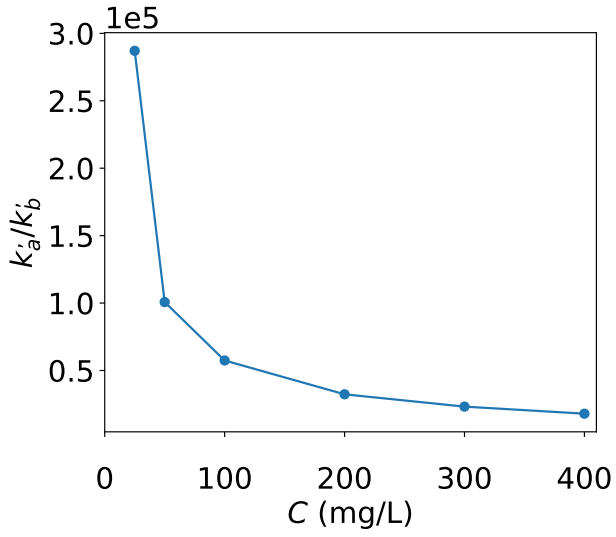

Figure 2.2: Calibrated $k_A^{'}/k_B^{'}$ values as a function of C for the Set A experiments of Tran et al. [2018].

2.2 Equilibrium properties of W98

A better understanding, at least in part, of what needs to be modified with the W98 model to make it more applicable to a broader range of environmental conditions can be obtained by examining the steady-state (or equilibrium) solution of the W98 model and the way in which values of $p = 3 - n_f$ and $q = 0.5$ were originally selected.

Solution to Equation 1.10 yields $D = D(t)$ starting from an initial floc size of D_0. As time progresses, Equation 1.10 always pushes the floc size towards some equilibrium value, D_e, where the aggregation and breakup rate terms are balanced, i.e., $dD/Dt = 0$ or $A = B$. If D_0 is larger than D_e, the movement towards the equilibrium condition will occur through net breakup. When D_0 is smaller than D_e, the movement towards the equilibrium condition occurs through net aggregation. Winterwerp [1998] used knowledge about the behavior of D_e in an attempt to provide physically meaningful values for p and q. We elaborate on this line of reasoning here because an understanding of the process taken to obtain the values of p and q typically used in the W98 model helps to motivate and explain the modifications we propose later on.

Taking $dD/Dt = 0$ at $D = D_e$ in Equation 1.10, and assuming that $D_e \gg D_p$, gives the following relation for the equilibrium floc size:

$$D_e = \left[\left(\frac{k_A'}{k_B'} \frac{1}{\rho_s} \right) D_p^{n_f+p-3} C \left(\frac{\mu}{F_y} \right)^{-q} G^{-q} \right]^{1/(2q+p+n_f-3)} \tag{2.1}$$

Many studies have shown that the equilibrium floc size is proportional to the Kolmogorov microscale, or, equivalently, that $D_e \propto G^{-1/2}$ [Eisma, 1986, Scully and Friedrichs, 2007, Verney et al., 2009]. To ensure that this proportionality held, Winterwerp [1998] noted that p should be equal to $3 - n_f$ (or that $p + n_f - 3 = 0$). The reason for this is that Equation 2.1 shows that,

$$D_e \propto G^{-q/(2q+p+n_f-3)} \tag{2.2}$$

Requiring that $p = 3 - n_f$ allows Equation 2.1 to reduced to:

$$D_e = \left(\frac{k_A'}{k_B'}\frac{1}{\rho_s}\right)^{1/2q}\left(\frac{\mu}{F_y}\right)^{-1/2} C^{1/2q} G^{-1/2} \tag{2.3}$$

To propose a reasonable value for q, Winterwerp [1998] used the net suspension settling velocity data from stagnant column tests that are typically used to produce empirical floc settling velocity equations as described in the introduction [e.g., Hwang, 1989]. Such data shows that for concentrations less than those that produce hindered settling, the net suspension settling velocity is linearly related to the suspended sediment concentration, $w_{s:net} \propto C$. Taking $D_e \propto w_{s:net}$, Winterwerp [1998] reasoned that q be set to 0.5 to ensure that $D_e \propto C$ (Eq. 2.3). It is worth noting here that with stagnant column tests, differential settling drives flocculation (something the W98 model does not consider) and there is no turbulent shear generating hydraulic stress on the flocs.

Using the value for $n_f = 2$, $p = 3 - n_f = 1$ and $q = 0.5$, an equation for the

equilibrium floc size based on the W98 can be proposed as follows:

$$D_e = D_p + \left(\frac{k_A^{'}}{k_B^{'}}\frac{1}{\rho_s}\right)\left(\frac{\mu}{F_y}\right)^{-1/2} CG^{-1/2} \tag{2.4}$$

Here, D_p has been added back to the equation to ensure that $D_e \neq 0$ for very high shear or very low concentration. Equation 2.4 is equivalent to equation 27 of Winterwerp [1998] paper,

$$D_e = D_p + \frac{k_A C}{k_B\sqrt{G}} \tag{2.5}$$

where k_A and k_B are defined as:

$$k_A = \frac{k_A^{'}}{n_f}\frac{D_p^{n_f-3}}{\rho_s} \tag{2.6}$$

and,

$$k_B = \frac{k_B^{'}}{n_f} D_p^{-p}\left(\frac{\mu}{F_y}\right)^{q} \tag{2.7}$$

While $D_e \propto C$ in Equation 2.5, note that the general case in the original W98 formulation is that $D_e \propto C^{-1/2q}$, with q being the power for the ratio of (τ_t/τ_y) in the floc breakup kernel (Eq. 1.10); the larger q is, the larger the rate of floc breakup.

2.3 A New Formulation of Floc Breakup

The need to recalibrate the W98 model $k_A^{'}$ and $k_B^{'}$ coefficients for each change in concentration limits the use of the W98 model in predictive sediment transport modeling, and it suggests that perhaps there is something in the development of the model that does not accurately capture the first-order physics. We propose that the following two assumptions in the W98 formulation lead to the undesirable behavior: (1) that flocs in the solution are always smaller than the Kolmogorov microscale, and (2) that $D_e \propto C$.

One consistent observation among various laboratory and field studies is that the maximum floc size is bounded by the Kolmogorov microscale, η [Parker et al., 1972, Coufort et al., 2005, Kumar et al., 2010, Cartwright et al., 2011, Braithwaite et al., 2012]. Parker et al. [1972] proposed that this bounding of the flocs size by the scale of η is due to a change in the functionality of the breakup rate with G around $D \approx \eta$. For $D < \eta$, Parker et al. [1972] states that the breakup rate should be proportional to G^2; whereas for $D > \eta$ the breakup rate goes with G^4. A change in breakup-rate functionality such as this around $D \approx \eta$ is not present in the W98 model. And, as such, D is not forced to be limited by η. For example, if we calculate D_e from either Equation 2.4 or 2.5 using the $k_A^{'}/k_B^{'}$ values obtained by calibrating the W98 model at a lower concentration, e.g., $C = 50$ mg/L, we see that the calculated D_e increases linearly with respect to C without regard for η (Fig. 2.3). This behavior results in D_e exceeding 6η by the time concentration gets into the 500 mg/L range, which is physically unrealistic.

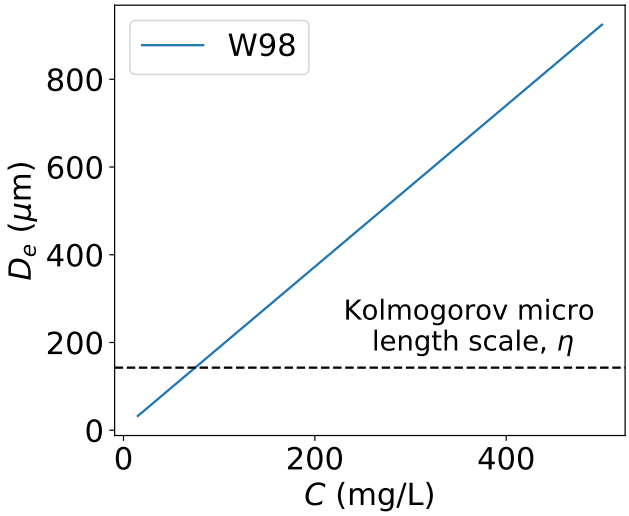

Figure 2.3: A prediction of the equilibrium floc size, D_e, over a reasonable range of concentrations using the W98 equilibrium size model (Eqs. 2.4 or 2.5) and the $k_A^{'}/k_B^{'}$ ratio obtained with the data for $C = 50$ mg/L from the Tran et al. [2018] dataset.

To remedy this limitation, we propose a simple modification to the Winterwerp [1998] floc erosion rate model that is a function of D/η. We start with the same breakup kernel (Eq. 1.12), but propose that q should be a function of D/η. Based on trial and error, we propose the following linear model for q,

$$q = c_1 + c_2 \frac{D}{\eta} \tag{2.8}$$

where c_1 and c_2 are constant coefficients. For the case when $D \ll \eta$, Equation 2.8 reduces to $q = c_1$ (which is similar to the original W98 formulation). However, as D approaches η, q increases from this baseline value of $q = c_1$ and therefore limits floc size. Equation 2.8 can be used along with the primary equations that come from the W98 model (Eqs. 1.10 and 2.3) to predict either the time dependent or equilibrium floc size, and it is the

major outcome of this study.

Input values for the new model are the same as those for the W98 model with the exception that c_1 and c_2 must now be defined in place of the original constant coefficient for q. In keeping with W98, we take $p = 3 - n_f$ to ensure that D_e is proportional to $1/\sqrt{G}$ (or $D_e \propto \eta$). We also propose that it is reasonable to take $c_1 = 0.5$ so that the new model reduces back to W98 when $D \ll \eta$ (as would be the case in a stagnant column of water where $\eta \to \infty$).

2.4 New model functionality

In this section we explore the functionality of the new model and how changes in the c_2 coefficient impact the time dependent and equilibrium size solutions for floc size. To better explore the impact of Equation 2.8 and specific values of c_2 on the solution, it is useful to introduce the concept of "spread" between calculated equilibrium sizes at different concentrations. For the purpose of this paper, we define the spread, ΔD_e, as being $\Delta D_e = D_e(C = 400 \text{ mg/L}) - D_e(C = 50 \text{ mg/L})$. For example, the difference between D_e in Figure 2.1A and 2.1B with the W98 model would be the spread, with $\Delta D_e \approx 600$ μm. It is this $\Delta D_e = \Delta D_e(C)$ that the W98 model tends to over predict.

For these calculations we have taken $G = 50$ s^{-1}, $n_f = 2$, $F_y = 10^{-10}$ N, $k_A^{'} = 0.45$, $k_B^{'} = 1.16\text{E}{-6}$, $\rho_s = 2650$ kg/m^3, $\mu = 1 \times 10^{-3}$ N-s/m^2, and $D_p = 5$ μm as the baseline condition. We then explore the model solution under different values of c_1 and c_2. To

start, we select $c_1 = 0.5$ and explore the influence of c_2 values on both D_e and the spread, ΔD_e. Figure 2.4 shows that both quantities decrease with an increase in c_2, and that c_2 strongly influences the spread. While we do not show all of the results here, we have empirically found that the c_2 parameter exerts far more control on the spread than does c_1, n_f (and hence p also), F_y, or D_p. In fact, it is impossible to obtain the ΔD_e spread observed in Tran et al. [2018], $\Delta D_e = 41$ μm, without the introduction of Equation 2.8 and an appropriate value for c_2.

We have selected $c_2 = 1.5$ as the coefficient value to use along with $c_1 = 0.5$ because a c_2 value of 1.5 yields a ΔD_e that matches the data from Tran et al. [2018], and because the pairing of $c_1 = 0.5$ and $c_2 = 1.5$ produces reasonable equilibrium floc sizes across a broad range of concentration values. Figure 2.5 shows the calculated value of D_e/η for a range of c_2 values and concentrations, ranging from $C = 0.025$ g/L up to 50 g/L.

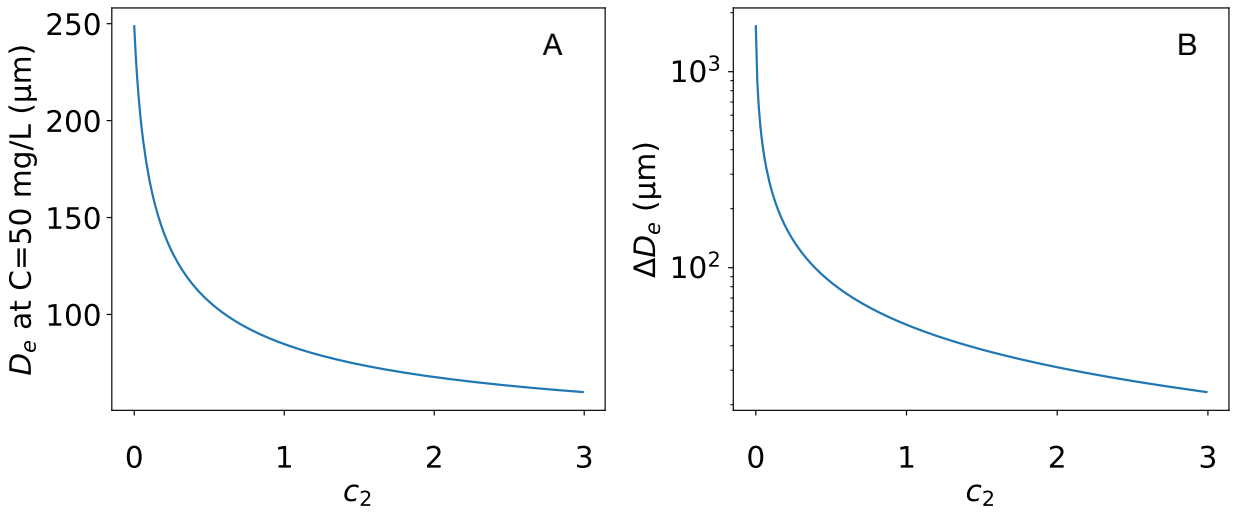

Figure 2.4: Change in the equilibrium floc size, D_e, and the difference between the predicted equilibrium floc size at $C = 50$ mg/L and $C = 400$ mg/L.

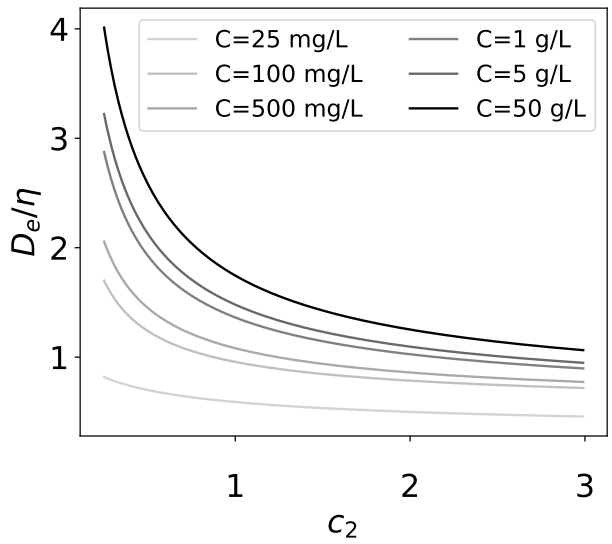

Figure 2.5: Equilibrium floc size scaled with the Kolmogorov microscale for a range of c_2 values and suspended sediment concentrations

In general, the solution of Equation 1.10 with q defined using Equation 2.8 produces floc time series that take the same basic form as the original W98 model (Fig. 2.6). The difference is that making q a function of D/η, rather than a constant, means that the new formulation of q leads to a strong increase in the breakup rate kernel as D approaches η. Figure 2.7 shows the ratio of the breakup kernel (Eq. 1.12) using the new definition of q (Eq. 2.8) to that with the original $q = 0.5$. The two breakup rates are nearly the same until approximately η. From here on, the breakup rate with the new definition of q begins to increase past that of the original formulation; this is especially true for $D > 4\eta/3$. The outcome of this new formulation is that the equilibrium floc sizes are limited by the size of η. For example, Figure 2.8 compares the D_e value calculated from both the original W98 formulation and the modification to η under turbulent shear rate values from $G = 5$ to 90 s^{-1}.

It also means that the functionality between D_e and C is dependent on D and G (Eq. 2.3). For example, if $D_e \ll \eta = \sqrt{\nu/G}$ then $D_e \propto C$ as it was in the W98 model. However, as D_e approaches η, this functionality with C becomes modified by the turbulent shear rate. The same is true for the ratio of $k_A^{'}$ over $k_B^{'}$ (Eq. 2.3).

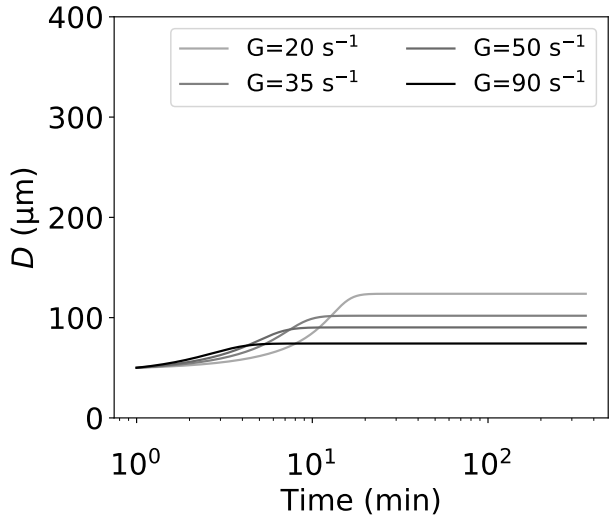

Figure 2.6: Solution of Equation 1.10 with q defined by Equation 2.8 for different shear rates. In this case, all parameters other than G are set to the baseline values as defined in the text.

2.5 Model Testing

We now use the new formulation of q in the W98 model to further explore the ability of the model to capture the trends observed in the experimental study of Tran et al. [2018]. Two sets of experiments were performed by Tran et al. [2018]. The first (Set A) measured the growth of flocs from a primary particle state up to an equilibrium condition under a range of suspended sediment concentration (i.e., $C = 15$, 25, 50, 100, 200, and 400 mg/L);

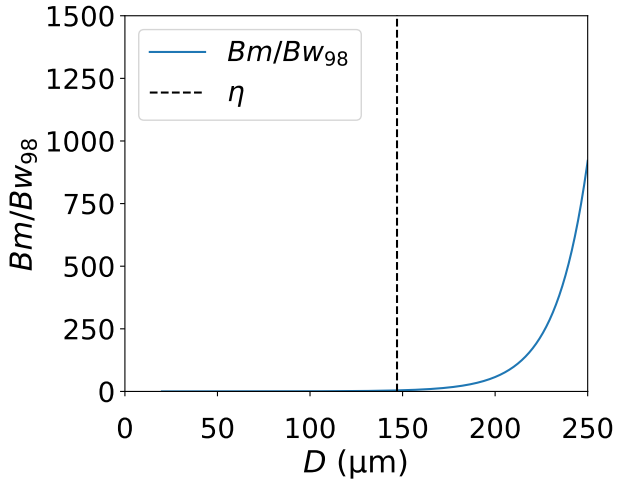

Figure 2.7: Ratio of the breakup rate kernel using the new model for q, Bm, compared to the original constant q value in the W98 model, Bw_{98}.

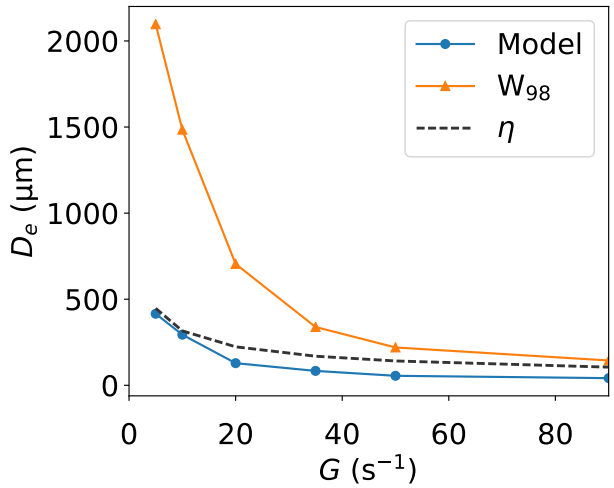

Figure 2.8: Comparison between D_e values calculated using the original W98 model and the new model to the Kolmogorov microscale, η, over a range of turbulent shear conditions.

in all runs, G was held constant at 50 s^{-1} to prevent settling. The data at $C = 50$ and 400 mg/L that was introduced in section 2.1 came from the Set A experiments. In the second set of experiments (Set B), flocs were first allowed to grow up to their equilibrium size in a concentration of 400 mg/L. The concentration in the tank was then decreased at a

steady rate down to a concentration of $C = 25$ mg/L. This was done three times with different rates of decrease from 400 to 50 mg/L (i.e., 50, 100, and 200 min) at a turbulent shearing condition of $G = 50$ s^{-1}. Floc sizes were measured within the suspensions for both Set A and Set B at all points in time using a floc camera [Tran et al., 2018].

To test the new model for q, we calibrated the $k_A^{'}$ and $k_B^{'}$ coefficients to the time series data from Set A of Tran et al. [2018] at $C = 50$ mg/L. We then used the calibrated $k_A^{'}$ and $k_B^{'}$ from this experiment to predict the floc sizes in concentrations below and above $C = 50$ mg/L without recalibrating the $k_A^{'}$ and $k_B^{'}$ coefficients. Figure 2.9A shows the model calibrated to the $C = 50$ mg/L data, and Figure 2.9B shows a comparison between the measured data and model prediction for $C = 400$ mg/L. This comparison shows that the new model is able to reasonably predict the size of the flocs under different concentrations without recalibrating $k_A^{'}$ and $k_B^{'}$. Part of the reason for this is that $c_2 = 1.5$ was itself obtained to capture the observed spread between D_e at $C = 50$ and 400 mg/L. However, it is encouraging to see that the model was also able to predict the sizes associated with the intermediate concentrations (i.e., $C = 100$, and 200 mg/L) as well as the concentrations below $C = 50$ (i.e., $C = 15$ and 25 mg/L). In fact, the model does an excellent job of capturing the non-linear trend between the equilibrium floc size and the suspended sediment concentration that was observed in the Set A experiments of Tran et al. [2018] (Fig. 2.10).

The new model was also used to predict the change in floc size as a function of time varying concentration from the Set B experiments. To make these calculations,

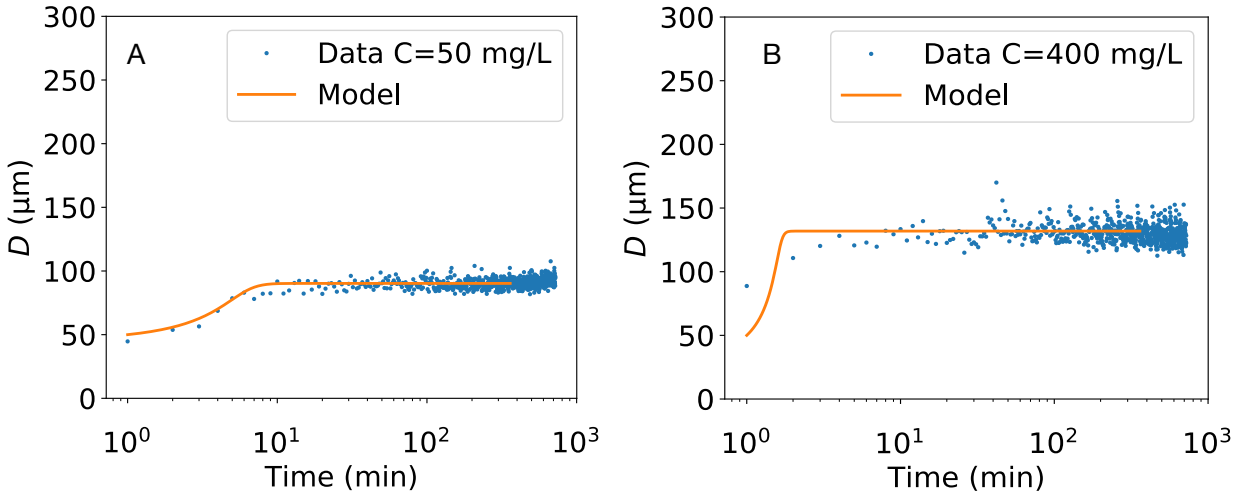

Figure 2.9: Comparison between the model and data from Tran et al. [2018] for (A) $C = 50$ mg/L and (B) $C = 400$ mg/L. $k_A^{'}$ and $k_B^{'}$ values were calibrated to the data at $C = 50$ mg/L and then used to predict the size $C = 400$ mg/L

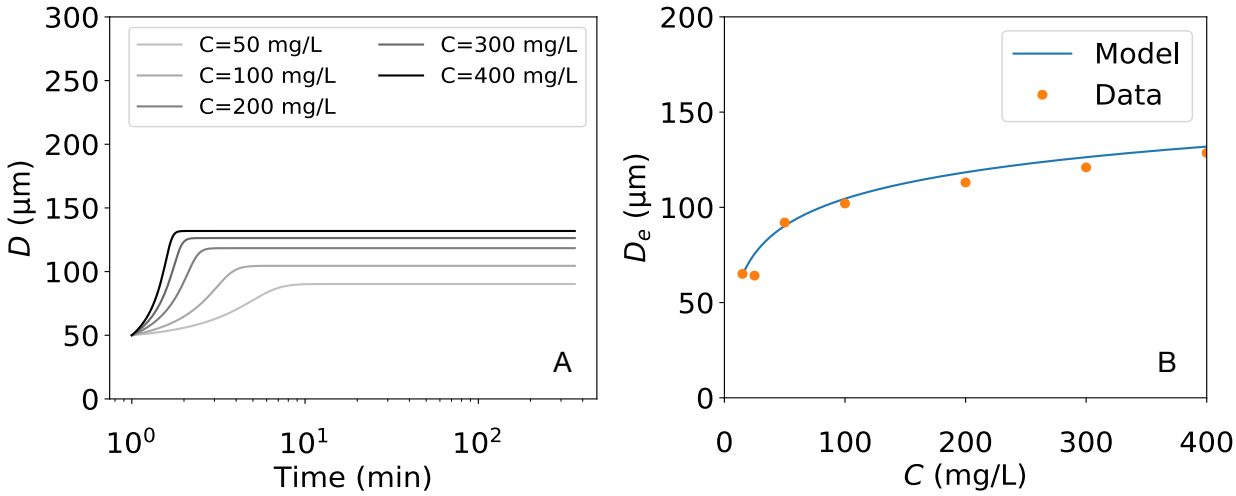

Figure 2.10: (A) Plot of the $D = D(t)$ solutions obtained with the new model using the $k_A^{'}$ and $k_B^{'}$ values obtained from the $C = 50$ mg/L data; and (B) plot of the measured and predicted equilibrium floc size.

we used the same $k_A^{'}$ and $k_B^{'}$ calibration values obtained from the $C = 50$ mg/L Set A experiment. We then set $D_0 \approx D_e$ for the condition of $G = 50$ s^{-1} and $C = 400$ mg/L, and used the measured concentration time series from the experiments to drive a time-

dependent response in the floc size through Equation 1.10 using Equation 2.8. Figure 2.11 shows the results from these calculations. The results are again highly encouraging as they show that the model is able to capture the time-dependent change in floc size due to a change in concentration without any recalibration of the k'_A and k'_B parameters.

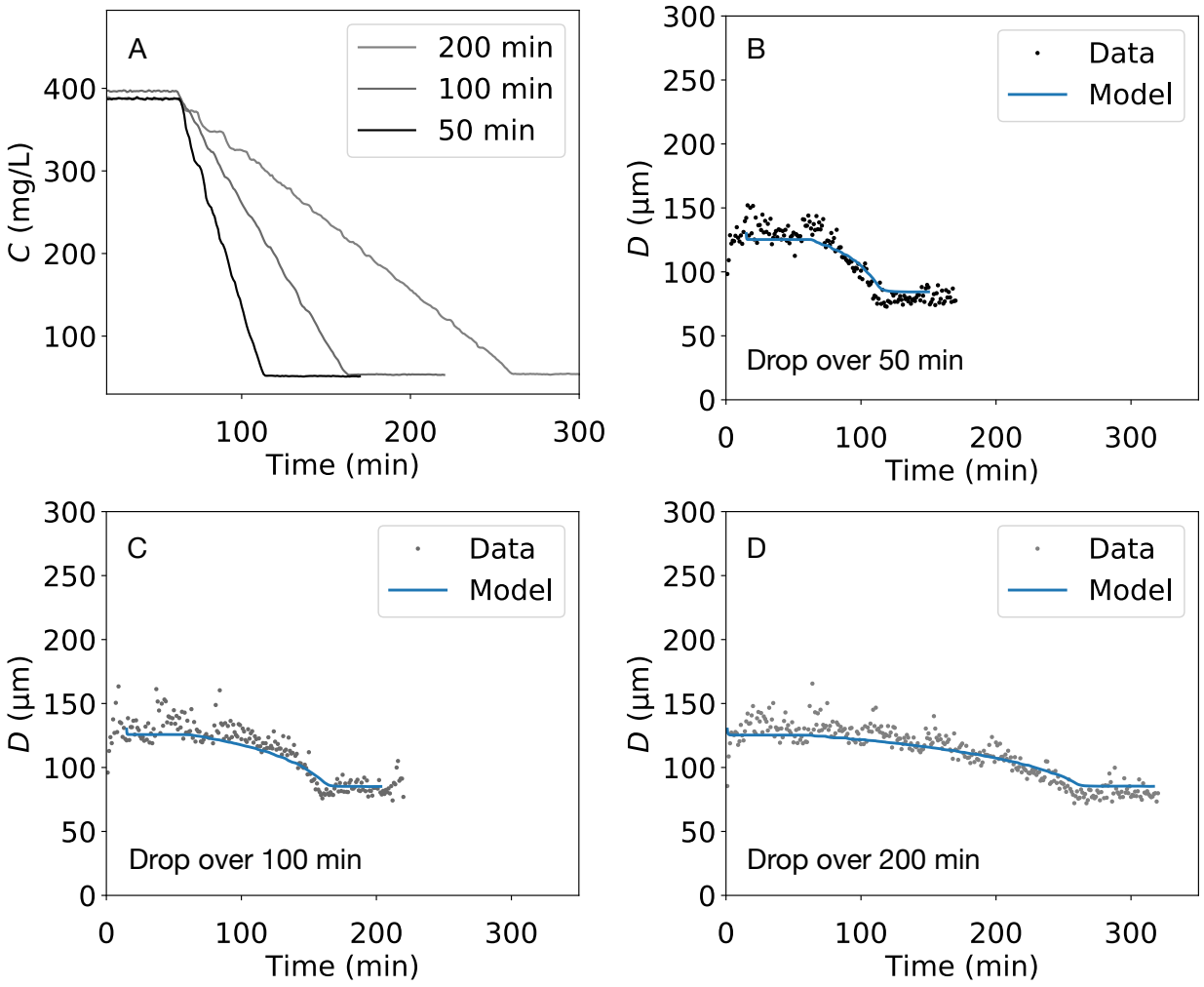

Figure 2.11: Experimental drop in C under conditions of constant G (panel A), and comparison between the experimental Set B data from Tran et al. [2018] and model for times of concentration decay from 400 to 50 mg/L of (B) 50 min, (C) 100 min, and (D) 200 min.

2.5.1 Field data

The laboratory tests described above lend themselves well to simple testing of the model behavior. This is because the same packet of fluid and sediment is measured with time while controlling variables such as C and G are isolated and systematically varied. Similar testing of the floc model with field observations is more challenging. In the field, G and C typically co-vary and sediment moves into and out of a particular sampling location through advection, settling, and resuspension. Therefore, proper testing of the model can only be done using an Eulerian formulation of the floc size model coupled with an advection-diffusion equation for suspended sediment in a 2 or 3D hydrodynamic model of the field site of interest. Furthermore, time series measurements of flocs are most commonly obtained with a Sequoia LISST [e.g., Markussen and Andersen, 2014]. The LISST instrument provides suspended particle size distributions using laser diffraction and therefore can yield slightly different floc sizes than image based techniques such as the one used in the experiments described above. Nevertheless, we compare the model here to field observations to show the reasonableness of the new formulation.

For testing of the model, we extracted time series data of average measured particles size, suspended sediment concentration, and fluid velocity from three tidally influenced field sites in the studies of: Markussen and Andersen [2014] (measurements made in the Danish Wadden Sea), and Schwarz et al. [2017] (measurements made in a brackish intertidal creek of the Scheldt estuary in the Netherlands). These two studies were

selected because they presented colocated, continuous time series of suspended particle size, C, and velocity, U; all particle size measurements were made with a LISST-100, and flocculation was suspected as a key driver of measured variation in the suspended aggregate size in all cases. The particular time windows from which data was extracted in each study was: t = 4:12 on 1/16/2011 to 18:42 on 1/17/2011 for Markussen and Andersen [2014]; and t = 10:22 to 14:38 on May 13, 2015 for Schwarz et al. [2017]. The extracted data from each study was then interpolated to produce evenly spaced time series to use in the integration of Equation 1.10. Each series was also shifted so that the first data point corresponded to $t = 0$ min.

To perform the integration, the extracted velocity time series data had to be converted to $G = G(t)$. With turbulence modeling, G can be obtained directly from the dissipation rate of turbulent kinetic energy, ϵ. However, here we estimate ϵ using the measured velocity time series $U = U(t)$. To do this, we couple the proportionality that should exist between ϵ and u_* (i.e., $\epsilon \propto u_*^3$) when production of turbulent kinetic energy is balanced by dissipation [Nezu and Nakagawa, 1993], and the proportionality between u_* and U (i.e., $u_* \propto U$). Doing so gives in $G \propto \sqrt{\mid U^3 \mid / \nu}$. Based on the velocity time series from the three field studies and reported ranges of G in estuaries, we have selected $G = 0.075\sqrt{\mid U^3 \mid / \nu}$ as a reasonable estimate of G for the three sites (Fig. 2.12). Using this values yields G up to 40 to 50 s^{-1} for U up to 0.8 m/s in the Wadden Sea [Markussen and Andersen, 2014], and G up to 15 to 20 s^{-1} for U up to 0.4 m/s in the Scheldt estuary [Schwarz et al., 2017]. While these values of G may not be entirely accurate, the time

series in G should be reflective of the first-order behavior and therefore suitable for using to examine the floc model behavior.

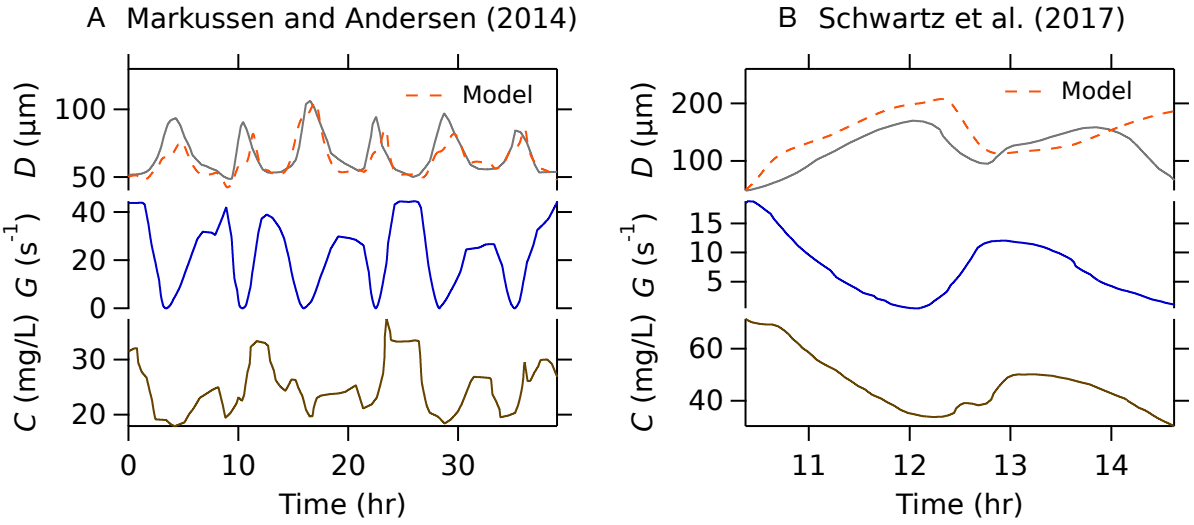

Figure 2.12: Comparison between modeled and observed suspended particle sizes at three tidally influenced field locations. All times in the studies have been shifted to start at time equals zero hours to better reflect the different time scales involved in each study. For Markussen and Andersen [2014] and Schwarz et al. [2017] the measured velocity ranged from -0.7 to 0.8 m/s and $\approx$ 0 to 0.4 m/s respectively during the time window displayed.

The following coefficient values were used in all calculations of $D = D(t)$: $c_2 = 0.5$, $c_2 = 1.5$, $n_f = 2$, $D_p = 7$ μm, $F_y = 10^{-10}$, and D_0 equal to the size of the measured floc at the start of the integration. The initial $k_A^{'}$ and $k_B^{'}$ were set to those used in the laboratory study ($k_A^{'} = 0.45$ and $k_B^{'} = 1.16\text{E-}6$). Updated $k_A^{'}$ and $k_B^{'}$ values for each case were then found by trial and error to produce a reasonable match between the observations and predictions (Fig. 2.12). A value of $k_A^{'} = 0.5$ and $k_B^{'} = 5.0\text{E-}6$ worked reasonably well for the Markussen and Andersen [2014] data (Fig. 2.12A). These same values for $k_A^{'}$ and $k_B^{'}$ also produced comparable, yet poorer, results between the observations and

predictions for the Schwarz et al. [2017] case (Fig. 2.12B); however, no pairing of data $k_A^{'}$ and $k_B^{'}$ values was found to do much better. This is perhaps due in part to fact that the measured floc sizes are inversely related to G over most of the time series, but then decreases with G over the tail end of the time series.

Of the two test cases, the model was able to best predict the measured sizes of Markussen and Andersen [2014]. The reason for this is not entirely clear. Perhaps the flocs from the Wadden Sea are more strongly controlled by shear in the water column and less by deposition and resuspension and therefore the site better corresponds to the condition inherently assumed in applying Equation 1.10 to the time series of G and C without accounting for advection, settling, and resuspension.

2.6 Discussion

2.6.1 When is the shear limiting modification important to use?

When is it important to use the modification over the original W98 formulation for breakup? We suggest that the answer to this question is: whenever the equilibrium floc sizes are on the order fo the Kolmogorov microscale. If the equilibrium floc size is well below η, then the original and modified W98 breakup rate kernel predict the same rate. However, as floc sizes near that of η ($\eta/2 < D_e \leq \eta$), as they did in Tran et al. [2018], the modification becomes extremely important. For example, we calculate the change in floc

size and settling velocity of mud suspensions in an idealized tidal zone and an idealized river mouth plume using both the original W98 formulation and the modification. For the idealized tidal conditions, G and C both co-varied sinusoidally to mimic a tide cycle with one low and one high slackwater condition over a 6 hour period. G was set to vary between near 0 to 30 s^{-1}. Two C time series were used. One had $C_{avg} = 75$ mg/L ($\pm$ 30 mg/L) and the other $C_{avg} = 200$ mg/L ($\pm$ 80 mg/L). For all cases, $k_A^{'}$ and $k_B^{'}$ were set to the values obtained for the W98 and modified W98 model using the Set A experiment of Tran et al. [2018] for $C = 50$ mg/L (the same values that were used in all previous model testing). The output from these calculations is shown in Figure 2.13. Both models yield reasonable floc size time series for the case with $C_{avg} = 75$ mg/L, but the unmodified W98 model predicts unrealistically large values for D for $C_{avg} = 200$ mg/L.

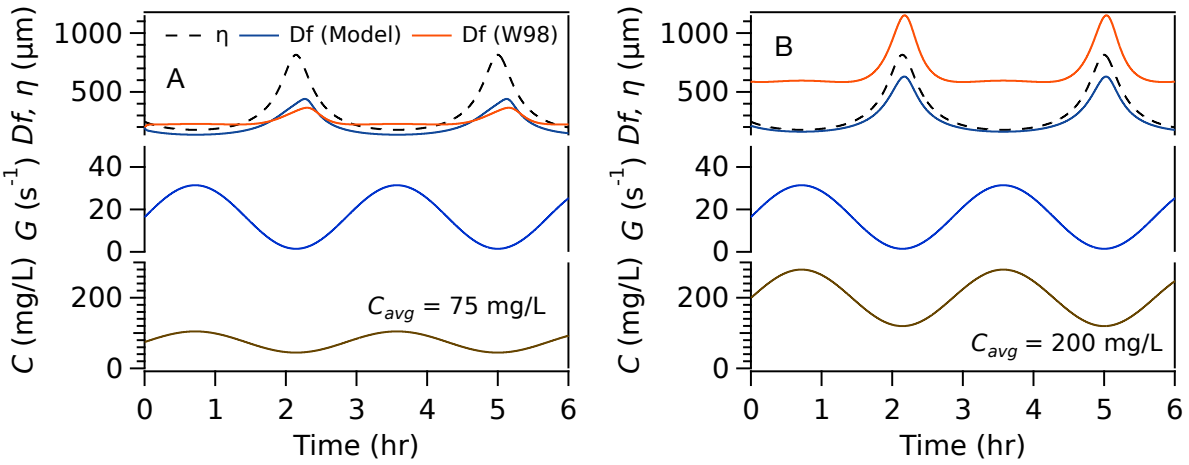

Figure 2.13: Floc size in an idealized tidal situation with covarying G and C. $k_A^{'}$ and $k_B^{'}$ values for the original and modified models were set based on the laboratory experiments conducted at $C = 50$ mg/L.

For the river-mouth plume, we used the steady-state model detailed in Strom and

Keyvani [2016] to make calculations of the estimated change in floc size and settling velocity as a packet of fluid traverses the discharge. The model is based on layer-averaged conservation of fluid momentum, mass, and volume and makes use of the Hetland [2010] lateral buoyant spread rate formulation. Equation 1.10 is solved along with the conservation equations using the assumption that $dt = dxU^{-1}$; note that velocity is not assumed to be constant, but is instead solved for in the system of equations along the length of the plume. Closure for G in Equation 1.10 is obtained using the relation suggested by Lane-Serff [1993], which again takes $\epsilon \propto U^3$. A mass conservation equation is also solved for the sediment in the plume. In this equation, ambient clearwater fluid is allowed to entrain across the bottom of the plume and sediment settles from the base of the plume at a rate of Cw_s. Settling velocity, w_s is calculated using the predicted floc size with the assumption that $n_f = 2$ and $D_p = 7$ μm with the floc settling velocity equation of Strom and Keyvani [2011].

The hydraulic conditions for the calculations, discharge $Q = 1750$ m^3/s with a river mouth width of 276 m, are based on those from the Merrimack River [Hetland and MacDonald, 2008]. These conditions produce $G = 44$ s^{-1} at the mouth down to $G = 1.5$ s^{-1} at 5 km out. Calculations were run with many different boundary conditions for the river mouth concentration. Here we present three, $C = 250$, 500, and 1000 mg/L to illustrate the trends (Fig. 2.14). In all cases, $k_A^{'}$ and $k_B^{'}$ for the W98 and modified W98 model were the same as in the tidal cycle calculations. The initial floc size, and hence floc settling velocity, at the mouth of the river was set equal to the equilibrium

floc size produced using the k'_A and k'_B values with the initial C and G values at the mouth. The primary outcome of these calculations is that the standard W98 model predicts very large floc sizes at the mouth (i.e., $D_0 = D_e =$ 480, 950, and 1900 μm for the three concentrations) that then decay in size throughout the plume due to the decrease in C along the length of the plume. The behavior shows that floc size is limited or controlled primarily be changes in C. However, the model with the modified breakup kernel predicts an increase in floc size and settling velocity (starting from $D_0 = D_e =$ 140, 160, and 170 μm) over the first 2.5 km followed by a decrease in floc size. The increase, followed by a decrease, in floc size predicted by the modification is reflective of the dominance of the decay in shear rate on the floc size over the initial portions of the plume followed by a dominance in the decay in concentration father out from shore.

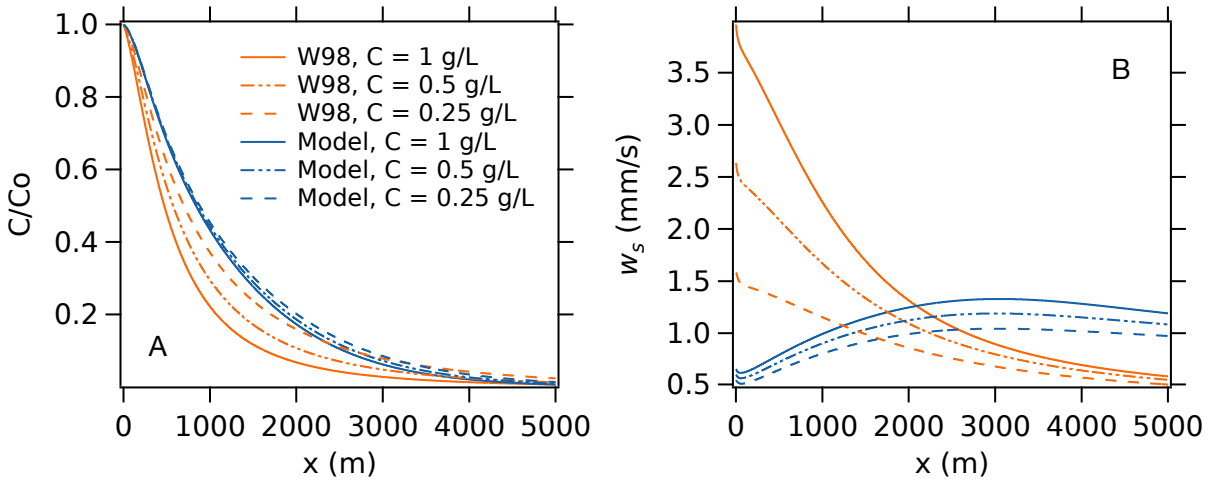

Figure 2.14: Calculated mud (A) concentrations and (B) floc settling velocities over the first 5 km of a river mouth discharge at three different initial concentrations.

The purpose of the idealized tidal and plume calculations is not to precisely predict floc sizes and settling velocities in a bay or plume. Rather, the purpose is to demonstrate

that using the W98 model without the shear limiting modification (Eq. 2.8) can lead to the prediction of unreasonably large flocs and an over-dependence of floc size on C in conditions outside of the range of model calibration.

For the calculations in this section, we used $k_A^{'}$ and $k_B^{'}$ values that were obtained from data generated in mixing tank experiments using a mixture of clay minerals. One might expect at first that the $k_A^{'}$ and $k_B^{'}$ values obtained from these experiments would be significantly different from those associated with natural mud mixtures and flow conditions. And, if this was the case, the question could be asked as to whether or not the trends in the simplified analysis are meaningful at all. However, the coefficient values obtained from the mixing tanks ($k_A^{'} = 0.45$ and $k_B^{'} = 1.16\text{E-}6$) were on the same order as those obtained through calibration of the the model to the data of Markussen and Andersen [2014] ($k_A^{'} = 0.5$ and $k_B^{'} = 5.0\text{E-}6$). We suspect that comparability between the laboratory and field settings is aided by the fact that C scales directly between the lab and field, and that the small-scale fluid motions that are thought to control particle collision and breakup in flocculation theory, characterized by G or ϵ, are comparable between the field and lab since information regarding the larger coherent flow structures is nearly lost at the smallest scales through the cascade process [Tennekes and Lumley, 1972, Tambo and Hozumi, 1979, McAnally and Mehta, 2000b, Serra et al., 2008, Tang et al., 2014].

2.6.2 Other proposed mechanisms to limit floc size with increases in concentration

In past multi-size class modeling efforts, the observation that D_e does not linearly increase with C across all values of C, and that the floc breakup rate increases near the equilibrium, has been explained in terms of an increase in floc breakup due to three-body collisions [Burban et al., 1989, McAnally and Mehta, 2000b]. In our paper, we have argued that the limit on floc size is set by fluid shear and not multi-body collisions of flocs that result in breakage. However, it is difficult to test whether an increase in ballistic collisions between flocs, an increased fluid stress, or some combination of the two is truly responsible for limiting floc size in energetic suspensions. To determine the causal mechanism, one would need to observe the breakup of a large number of flocs. Yet, no experimental technique exists, at least to our knowledge, to accomplish this task. Therefore, inferences about the causal mechanism must be made through modeling. In this paper we show that reasonable predictions of floc size can be obtained through a heuristic limiter on floc size that is based on the idea that the fluid stress imposed on the floc should be a function of the size of the floc relative to the Kolmogorov microscale.

2.6.3 Calibration parameters in floc modeling

Flocs are present in nearly every type of waterbody and flow that contains fine sediment with some amount of clay. Yet, it is rare for changes in floc size and their impact

on settling velocity to be accounted for in larger hydrodynamic and sediment transport models such as those used to determine Total Maximum Daily Loads (TMDLs) for various waterbodies. One impedance to including flocculation in larger models is that simple equilibrium or empirical floc settling velocity equations often miss many of the important dynamics, and that dynamic single-size class [Winterwerp, 1998], multi-size class [Verney et al., 2011, Shen and Maa, 2015], and distribution-based floc models [Maerz and Wirtz, 2009] all require the definition of model coefficients that are particular to a specific sediment and water column mixture. For example, the single-floc-size-class model of Winterwerp [1998], one needs at least to define values for $k_A^{'}$ and $k_B^{'}$ along with values for n_f and D_p; both of which, mathematically, influence the rate of growth and to a lesser extent the equilibrium size (Fig. 1.2). Therefore, to include flocculation dynamics, one needs data on floc size of a particular suspension as a function of driving parameter to determine reasonable values to use in the model.

Time series data of floc sizes is not easy to come by, and it is unreasonable to expect that floc size data can be collected across the full spectrum of flow and concentration conditions that may be experienced in any field scenario. Therefore, it would be advantageous if floc model calibration parameters, such as $k_A^{'}$ and $k_B^{'}$ in the W98 model, could be calibrated at one particular set of conditions (say in a laboratory), and then used across a much wider set of conditions than those for which the models were calibrated. However, testing of the ability of $k_A^{'}$ and $k_B^{'}$ determined from experiments at $C = 50$ mg/L using the original W98 formulation showed that the model drastically

over predicted floc sizes at higher concentrations. The goal of the work presented in this paper is to expand the range of applicability of W98 model by limiting floc size to the Kolmogorov microscale. Doing so produced a model that was better behaved across a wider range of concentrations.

2.7 Conclusions

The single-floc-size-class model of Winterwerp [1998] is an attractive choice for including floc dynamics in sediment transport models. The model has been shown to capture many of the first-order trends in floc growth and breakup, and it is easy to incorporate into transport models since it is driven by suspended sediment concentration and turbulent shearing, which is a function of the turbulent kinetic energy dissipation rate, ϵ, $G = \sqrt{\epsilon/\nu}$. However, the breakup rate equation used in the Winterwerp [1998] model assumes that flocs are always smaller than the Kolmogorov microscale, η, and that the equilibrium floc size increases linearly with suspended sediment concentration. These two assumptions couple to produce a model that can be very sensitive to changes in C, and one that often predicts floc sizes well in excess of η if it is used outside of the suspended sediment concentration for which the aggregation and breakup coefficients, $k_A^{'}$ and $k_B^{'}$, were obtained. This behavior limits the use of the Winterwerp [1998] formulation in predictive modeling where changes in C would be expected.

To address the shortcomings of the original Winterwerp [1998] model, we pro-

posed a simple modification to the breakup rate kernel. The modification results in a breakup rate that increases substantially relative to the original formulation as the floc size approaches, η. The simple modification is accomplished by taking q in the original formulation as a linear function of D/η instead of a constant (i.e., Eq. 2.8). Doing so provides at least two advances over previous formulations of the W98 equation. First, the modification limits the size of the flocs to that of the Kolmogorov microscale. The second is that the modification produces a model that is able to capture the time-dependent and steady-state functionalities between floc size and suspended sediment concentration across a range of concentration values; including conditions outside of those for which the model's aggregation and breakup coefficients were calibrated. Both of these advances are significant. The first is significant because nearly all laboratory and field studies of flocculation have concluded that the upper limit for floc size is approximately the Kolmogorov microscale (unless flocs are held together by biological binders). The second advance is significant because it means that the model can be used more confidently in a predictive way outside of the range of concentration conditions for which k_A' and k_B' were calibrated.

Chapter 3

Impact of Salinity on Flocculation

This chapter presents a set of experiments aimed at providing data needed to include the effects of salinity in the W98 model. Experiments were conducted at various salinity and concentration levels in order to quantify the effect of salinity on floc growth rate and equilibrium size. The M98 model, which can be found in the previous section, is then modified to account for salinity. It is hypothesized that an increase in salinity will increase the equilibrium floc size. This can then be accounted for by modifying the aggregation term of the M98 model.

3.1 Materials and Methods

Experiments were conducted at two concentrations of sediment (50 mg/L and 200 mg/L) at four different salinity levels (0, 2.5, 5, 10 PSU) to examine the influence of salinity on floc growth rate and equilibrium size. The sediment used in these experiments was an 80% kaolnite, 20% montmorillonite mixture used to mimic natural muds [Keyvani and Strom, 2014]. In these experiments, the sediment was first sonicated for 15 minutes in 100 mL of water. The sediment was then poured into a turbulent mixing tank and the flocs were allowed to grow to equilibrium for 12 hours at a constant G=50s^{-1}. The shear was then increased to 400s^{-1} for 30 minutes to break down the flocculated suspension into particles of the order of 15 microns and smaller. Lastly, the shear was decreased to 15s^{-1} and the flocs were allowed to grow until equilibrium for 6 hours with images collected every 2 seconds. Salinity was held constant in time for all experiments. Data collected for these experiments consisted of floc size distribution time series during periods of growth and at equilibrium. The experimental conditions are summarized in table 3.1. Additionally, for C=50 mg/L at S=2.5, 5, and 10 PSU, and C=200 mg/L at S=0, 2.5, 5, and 10 PSU, the shear rate was increased to G=95s^{-1} for 6 hours. Time series data was collected for the last 5 minutes in order to determine the equilibrium floc size.

C [mg/L]	S [PSU]
50	0
	2.5
	5
	10
200	0
	2.5
	5
	10

Table 3.1: Experimental conditions

3.1.1 Experimental Equipment

All experiments in this study were conducted in a 13 liter mixing tank with the dimensions of 27.5 x 27.5 x 25 cm. The shear rate for the mixing tank can be found using the equation for a paddle and tank geometry suggested by Logan [1999]:

$$G = \left(\frac{52.3 b_{d,p} A_p s^3 R_p^3}{\nu_w V_t} \right)^{1/2} \tag{3.1}$$

where $b_{d,p}$ is the drag coefficient, A_p is the paddle area in m^2, s is the paddle speed in rotations per minute, ν is the fluid kinematic viscosity (m^2/s), and V_T is the volume of the fluid in the mixing tank (m^3). The shear rate used in the study was G=15s^{-1}. This is a shear rate that can commonly be found in estuaries [Kumar et al., 2010]. An image of the experimental setup can seen in figure 3.1.

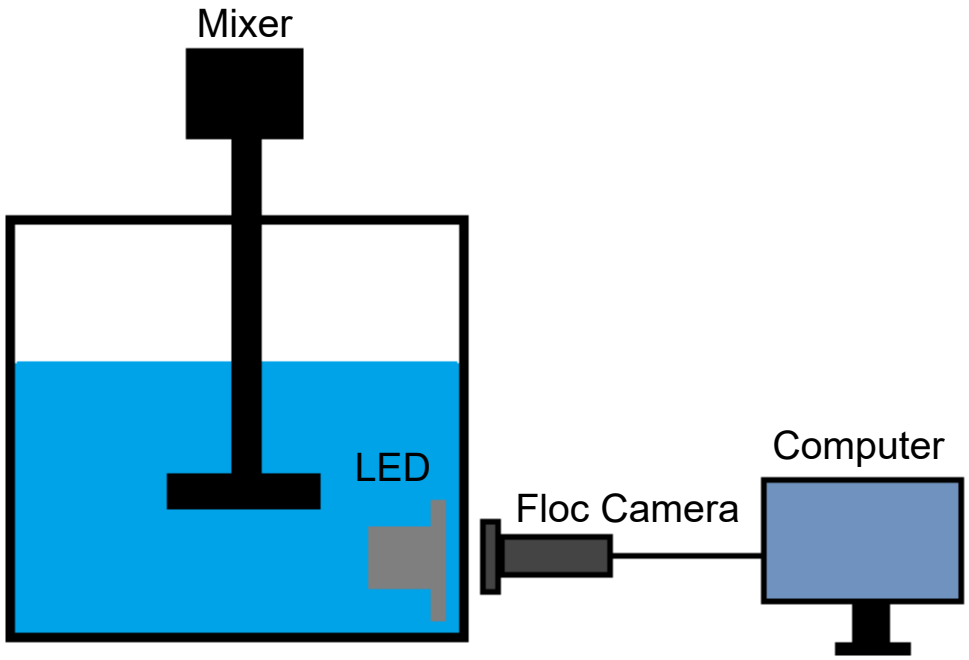

Figure 3.1: Experimental setup

In order to properly test my hypothesis regarding modifications to the W98 model for the incorporation of salinity effects, it is necessary to collect accurate measurements of floc sizes within the turbulent suspension. Using a camera and light system developed by Tran et al. [2018], images of flocs were collected every two seconds. These images were then processed using ImageJ and Matlab routines [Keyvani and Strom, 2013] to measure the size of in-focus flocs. A sample image can be seen in 3.2.

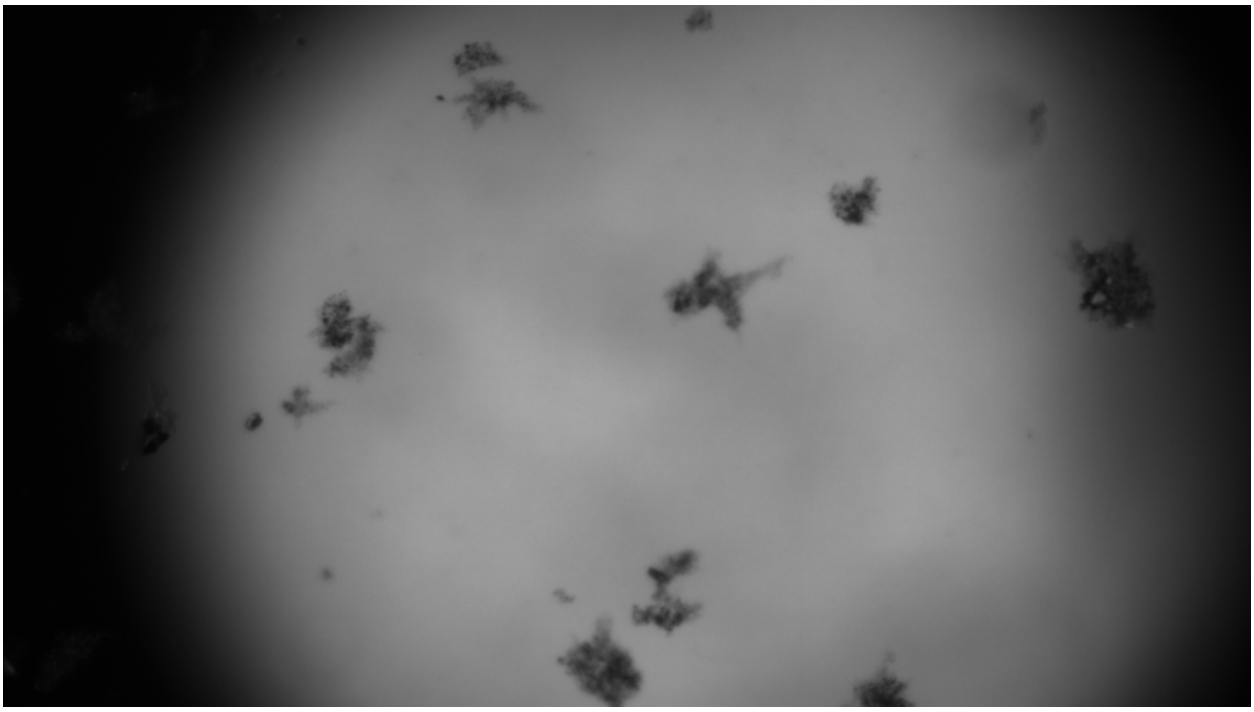

Figure 3.2: Example floc image

3.2 Experimental Results and Discussion

3.2.1 Results

Floc time series data for $G = 15s^{-1}$ can be seen in figure 3.3 for C = 50 mg/L and C = 200 mg/L. It is clear that adding salt does increase the equilibrium floc size (from 50 to 100 μm for C=50 mg/L and from 80 to 100 μm for C=200 mg/L; however, once S = 2.5 PSU there is little effect in equilibrium floc size. This salinity concentration is similar to the critical salinity levels found for montmorillonite by Ariathurai [1974]. This implies that once there is enough salt for flocculation to occur, the addition of more salt does not

affect the equilibrium floc size. This can be seen more clearly in the figure 3.4. It should be noted that due to the low shear rate, it is possible that some larger flocs settled out of suspension, thus, masking the effect of salinity on equilibrium floc size; however, the last 10 minutes of a similar experiment with a shear rate of G=95 s^{-1} (a shear rate in which there is no deposition), show that there is no apparent trend with salinity (fig. 3.5)

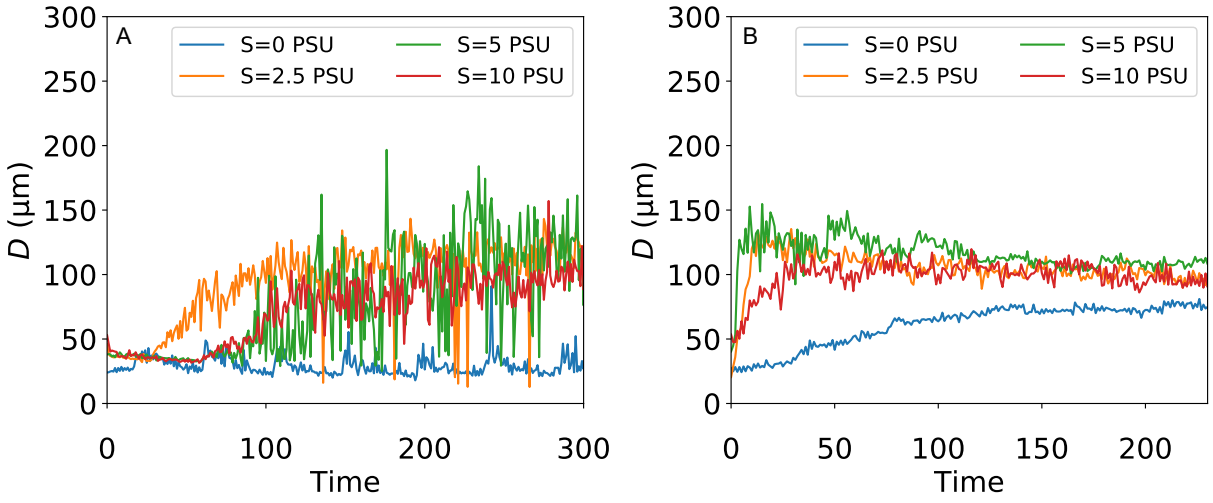

Figure 3.3: Results for prior shear G=15 s^{-1} (A) C=50 mg/L and (B) C=200 mg/L

Furthermore, it can be seen that the addition of salt decreases the time to equilibrium relative to the freshwater case; however, from 2.5 to 10 PSU, the time to equilibrium increases. This holds true for both 50 mg/L and 200 mg/L, with both concentrations showing the same trend of floc size and growth rate.

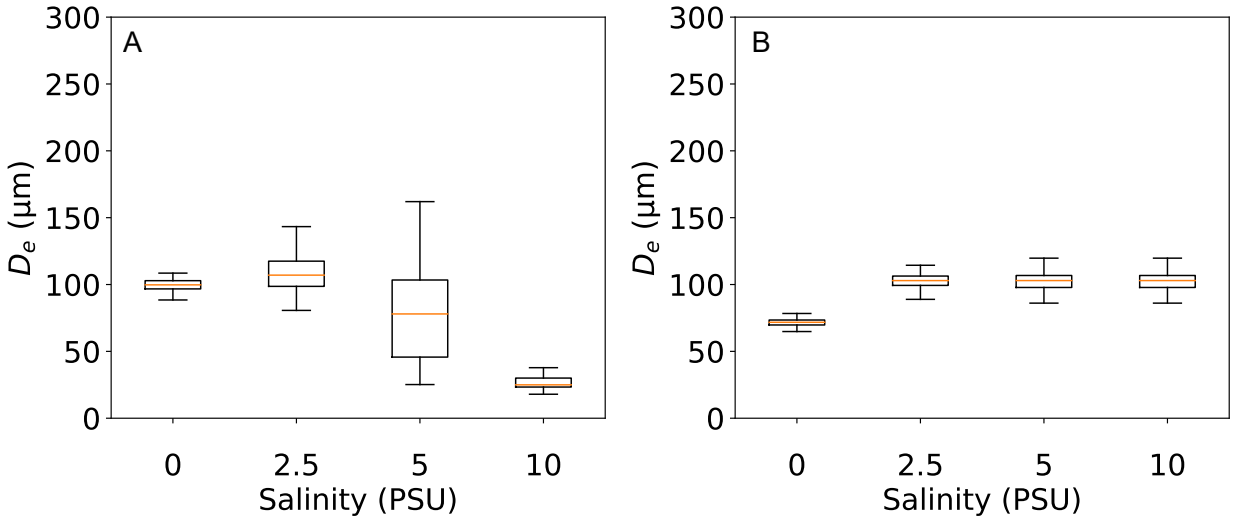

Figure 3.4: Results for D_e when G=15 s^{-1} (A) C=50 mg/L and (B) C=200 mg/L

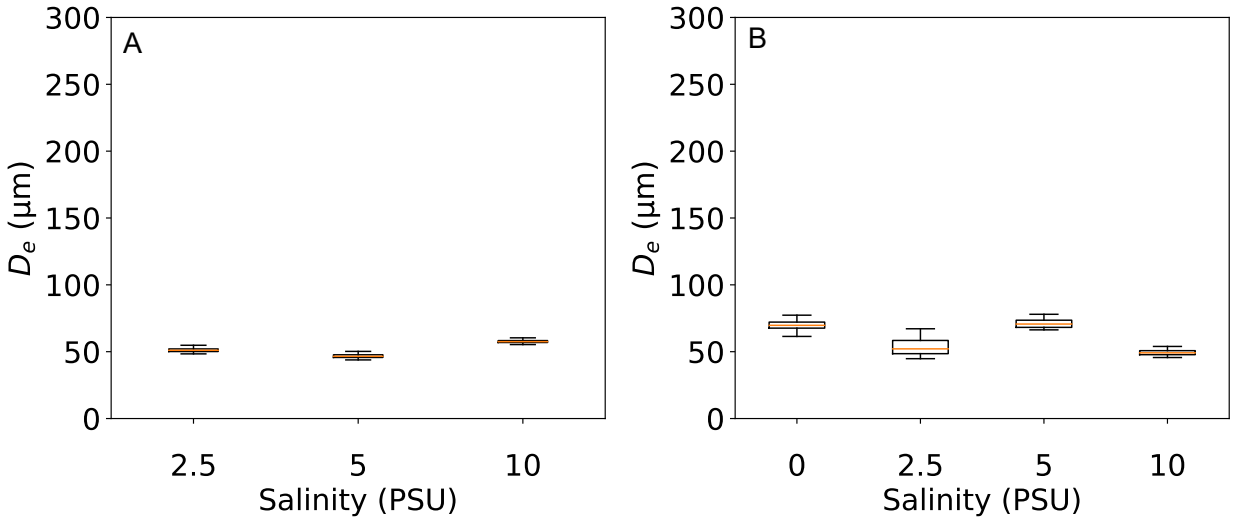

Figure 3.5: Results for D_e when G=95 s^{-1} (A) C=50 mg/L and (B) C=200 mg/L

3.2.2 Discussion

The finding that higher salinities can cause an increase in the time to equilibrium when going from a salinity of 2.5 to 10 PSU is different from what previous studies have found,

[Mietta, 2010, Burban et al., 1989]; however, it does agree with findings from Al Ani et al. [1991]. Al Ani et al. [1991] found that for salinities between 0-10 PSU, for the same size floc (500 μm), density increases as salinity increases. In a fractal aggregate framework, density can be related to the fractal dimension (eq. 1.5). Thus, an increase in density would be associated with an increase in the fractal dimension. As density of the floc goes up, so does the fractal dimension [Kranenburg, 1994]. As can be seen in figure 3.6, n_f has a very limited effect on the final equilibrium floc size for both the W98 and the M98 models; however, as n_f increases, the time to equilibrium also increases. This is due to more primary particles being packed into an aggregate of equivalent size.

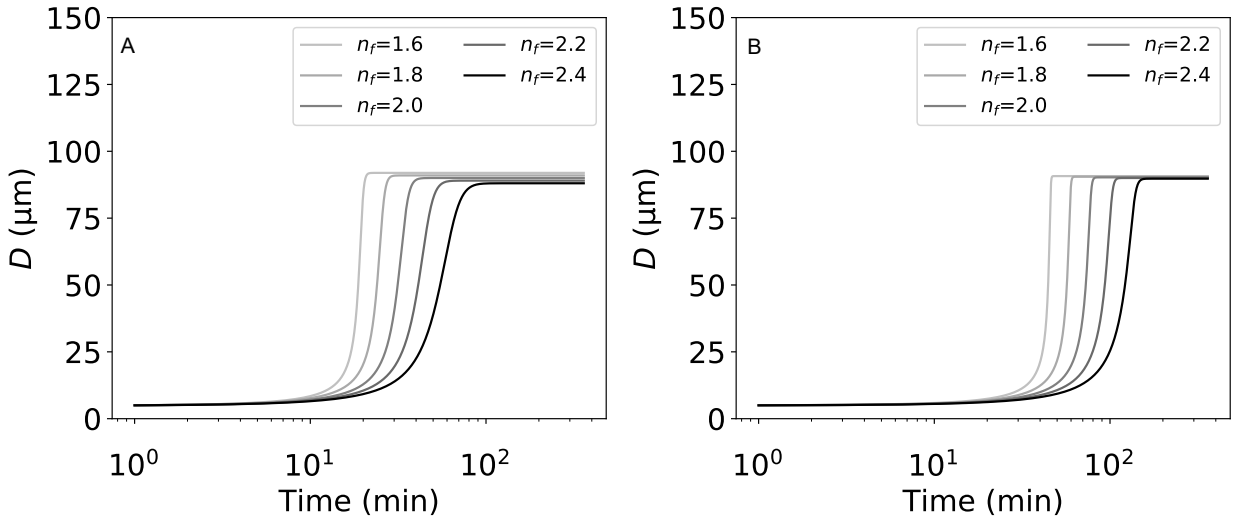

Figure 3.6: Effect of n_f on D for (A) W98 model (B) M98 model

The increase in fractal dimensions with salinity is supported by inspection of the images from experiments at different salinities (fig. 3.7). In figure 3.7, the images on the

left and the right were taken at the same second from S=2.5 PSU and S=10 PSU. Visually comparing the flocs in the two image columns, it appears that at S=10 PSU, the flocs are more dense. If this is true, then the flocs at S=10 PSU have a higher fractal dimension.

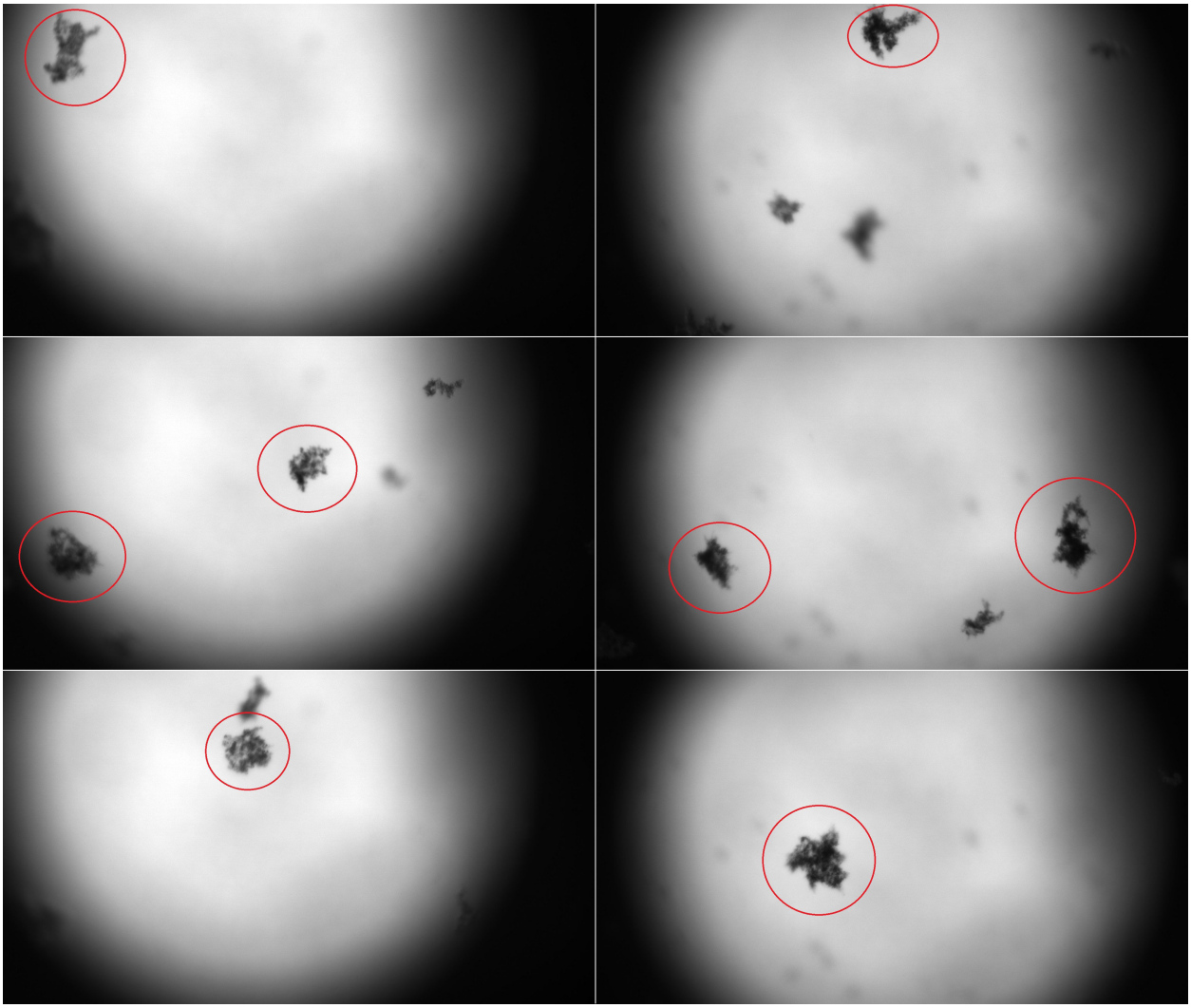

Figure 3.7: (A) Floc image at S=2.5 PSU (B) Floc image at S=10 PSU

An increase in n_f with an increase in S runs counter to classic aggregation theory, which would indicate that the ionic content in the water is increased, aggregation moves from being reaction limited to diffusive limited [Logan, 2012]. Essentially, when there

are no electrolytes in the water, aggregation is difficult because the energy barrier of the particles is strong, and thus, particles must statistically collide multiple times before aggregating; however, these collisions result in denser particles since particles can penetrate more deeply into an existing aggregate before sticking. Diffusion limited aggregation occurs in higher electrolyte solutions; aggregates form much more quickly, limited only by particle collision rate. These aggregates form less dense flocs with lower fractal dimensions [Logan, 2012].

Nevertheless, the observations from the experiments discussed above are not entirely unique. For example, Waite et al. [2001] found that increasing salinity resulted in n_f increasing. Waite et al. [2001] attempted to explain the observed increase in floc fractal dimension with increasing salinity by modifying a theory developed by Verwey and Overbeek [1948] and Derjaguin and Landau [1941] (i.e., the DVLO theory) to account for a second near range repulsive force. When particles are about 3 nm away from each other, particles adhere in accordance with the DVLO theory. This theory accounts for an electrical double layer repulsive forces and van der Waals attractive forces; however, at smaller separations, there is an additional repulsive force [Karaman et al., 1997]. Waite et al. [2001] proposed that while additional electrolytes did reduce longer range repulsive forces, the near range repulsive forces could have made aggregation more difficult, and thus, increased the compactness and fractal dimension. As the salinity levels tested in these experiments were low, it is possible that this secondary repulsive force is coming into play. As only salinities $\leq$ 10 PSU were tested, salinities at higher levels should

be examined further to determine at what level this secondary repulsive force becomes negligible (or whether that ever occurs).

3.3 Model Modifications

As shown in figure 3.6, at salinities from 2.5 PSU to 10 PSU, increasing n_f increases the time to equilibrium while having very little effect on the final equilibrium floc size. Such model behavior is in line with the experimental observations. Therefore, in order to incorporate the influence of salinity on the floc growth rate, a salinity term was introduced into n_f. This can be seen in equation 3.2.

$$n_f = n_{f,0} + \frac{\log(S)S^{0.8}}{c_3} \tag{3.2}$$

Where $n_{f,0}$ is the average fractal dimension for the specific sediment, in this case $n_{f,0} = 2.0$, and c_3 is a calibration coefficient for how influential salinity is on the growth rate of the floc. While log(S=0) is undefined, the limit of equation 3.2 as S approaches 0 is $n_{f,0}$ as the limit of $\log(S)S^{0.8}$ as S approaches 0 is 0. This equation was found by visually comparing a range of functionalities for n_f.

The results of the time series output of the M98 model can be seen in figure 3.8. For these particular experiments, the k'_a and k'_b values for the M98 model did have to be recalibrated between the C=50 mg/L and C=200 mg/L experiments (at C=50 mg/L:

k'_a=8.11 and k'_b=1.04E-04, and at C=200 mg/L: k'_a=12.6 and k'_b=4.64E-04) because as seen in figure 3.9, there was no change in equilibrium floc size between the two sets of experiments. While the Tran et al. [2018] found that increasing sediment concentration caused an increase in floc size used the same 80%/20% kaolnite and montmorillonite mixture, the kaolnite in these experiments was a different kaolnite than the kaolnite used in the Tran et al. [2018]. As discussed previously, different studies have found different results for the influence of concentration on equilibrium floc size depending on the sediment composition, and it is possible that these different sediment compositions caused the contradictory results. Additionally the time to equilibrium floc size decreases when salinity concentration increases. It has been found that at low salinity levels, $S \leq 10$, when concentration increases, fractal dimension decreases Burns et al. [1997]. Referring back to figure 3.6, decreasing n_f decreases the time to equilibrium. The new model will henceforth be referred to as S98.

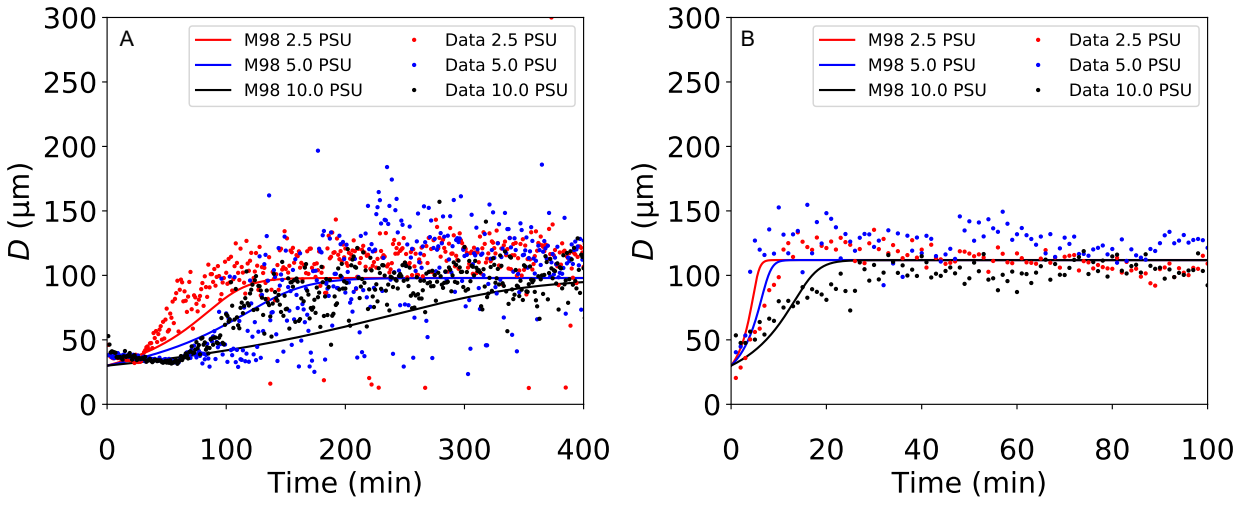

Figure 3.8: New n_f formulation for (A) C=50 mg/L (B) C=200 mg/L

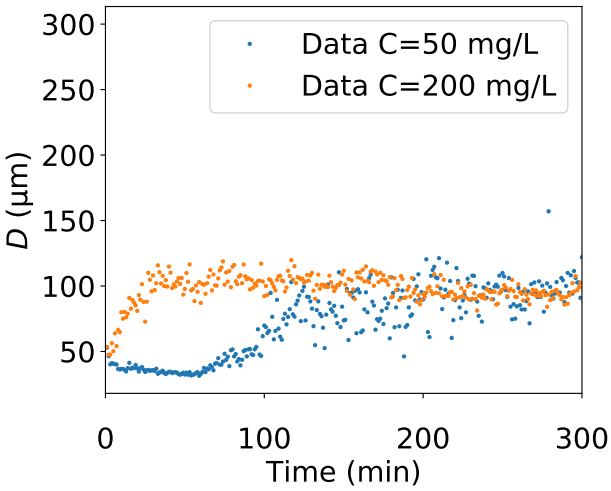

Figure 3.9: D for C=50 mg/L and C=200 mg/L at S=10 PSU

3.4 New Model Functionality

In this section we explore the functionality of the S98 model by looking at how changes in $n_{f,0}$ and c_3 impact the time dependent and equilibrium size solution. The influence of $n_{f,0}$ and c_3 will be determined by looking at how the growth rate changes. This will be done by comparing the flocs at a time of t=10 minutes to the the flocs at a time of t=10 minutes for the base case (equation 3.3).

$$\Delta D_{ratio,10} = \frac{D_{n_f,10}}{D_{base,10}} \tag{3.3}$$

Analysis of the S98 model will also observe how n_f changes with S. The influence of salinity on equilibrium floc size will not be discussed as changing n_f does not signifi-

cantly change the equilibrium floc size (figure 3.6). It is important to note that compared to a freshwater case, adding salt did significantly increase the equilibrium size; however, due to the lack of data for S=0-2.5 PSU, it is not possible quantify and model this impact.

As the model had to be recalibrated for C=50 mg/L and C=200 mg/L, the base case will be taken to be the one used for C=200 mg/L. In this case G=15 s^{-1}, $n_{f,0}$=1.0, c_3=50, C=200 mg/L, k'_a=12.6, and k'_b=4.64E-04.

Figure 3.10 shows how D at 10 minutes changes with changes in $n_{f,0}$ and c_3. It can be seen that increasing $n_{f,0}$ decreases D at 10 minutes. Since D is lower at 10 minutes, it take longer to reach equilibrium, thus demonstrating that increasing $n_{f,0}$ increases the time to equilibrium. It can also be seen that D increases with increases in c_3; that is that increasing c_3 decreases the time to equilibrium. Thus, increasing c_3 will decrease n_f. This is expected as the modification is a simple model for n_f which is put into the W98 model.

The influence of salinity on n_f can be seen in figure 3.11. While n_f for salinities from 0-10 PSU were looked at, it is important to note that the model is only applicable to salinities from 2.5-10 PSU. As salinity increases, n_f increases. This means that the growth rate decreases, which is what was seen in the results seen in figure 3.3.

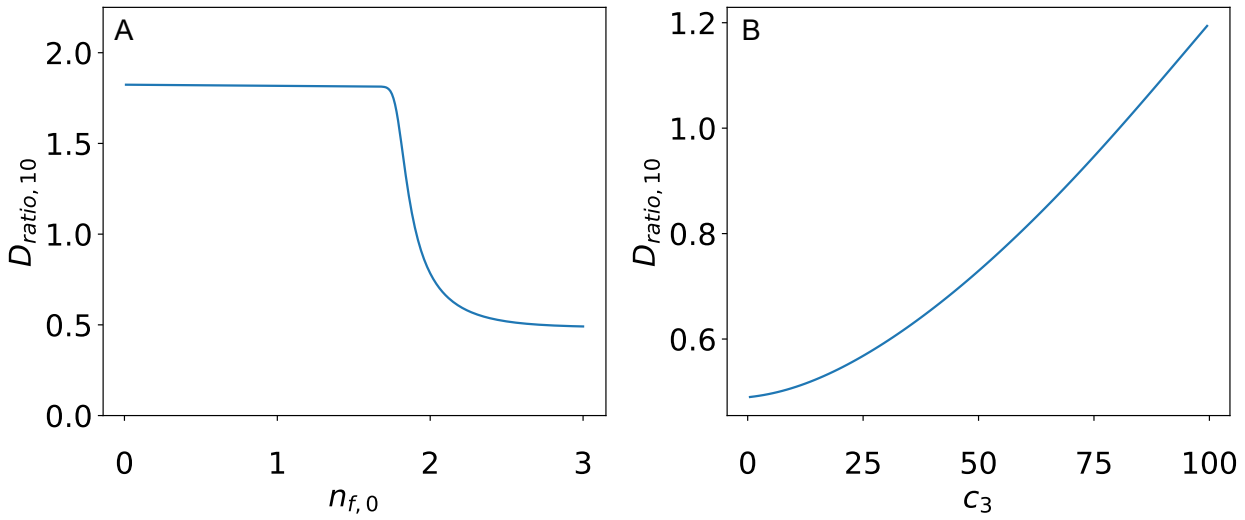

Figure 3.10: S98 model comparison for (A) changes in $n_{f,0}$ and (B) changes in c_3

3.5 Discussion and Concluding Remarks

Developing a model that can account for salinity variations is essential for estuarine environments. Using the Chesapeake Bay as an example, over the 200 miles from the head of the bay to the ocean, the salinity varies from 0 to 35 PSU CBP [2012]. While the very top of the bay, as well as the the part of the bay that opens to the ocean, have a relatively constant salinity, the salinity in the parts of the bay that experience changes due to the salt front can vary significantly [Partch and Smith, 1978]. Understanding the factors that influence flocculation in a salt wedge estuary is crucial in modeling estuarine turbidity maximum (ETM) zones as these zones only exist because of flocculation [Sanford et al., 2001]. ETM zones form due to the tidal forces pushing the salt front underneath the freshwater. The turbulence caused by the moving salt front causes the resuspension of

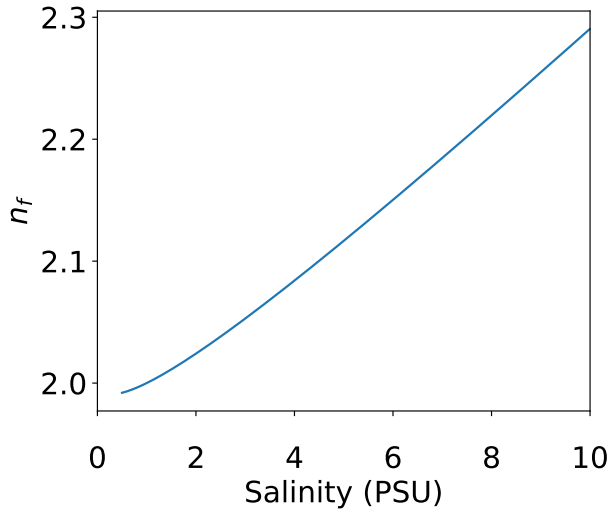

Figure 3.11: Effect of Salinity on n_f for S98 model.

sediment in the bed. The resuspended sediment is then flocculated and redistributed in the ETM [Geyer, 1993]. Additionally, Xu et al. [2010] found that flocculation plays a key role in the generation of strong tidal asymmetrical variations in suspended sediment concentration (SSC) of the Chesapeake Bay. If flocculation is accounted for, the tidally averaged sediment accumulation is small. Conversely if there is no flocculation, the suspended sediment is trapped at the salt front [Xu et al., 2010].

As the salt front is constantly moving, the salinity within the zone of movement is changing in both lengthwise and depthwise directions [CBP, 2012]. The model developed in this study can help improve larger sediment transport models by incorporating a changing salinity factor into the flocculation model.

Chapter 4

Conclusion

4.1 Objectives and Hypotheses

In regards to the first objective, to improve the behavior of the W98 model across a spectrum of suspended sediment concentration values, it was hypothesized that floc size is limited, approximately, by the Kolmogorov microscale. This was confirmed using existing experimental data and incorporated into a modified Winterwerp [1998] model, M98.

In regards to the second objective,to introduce to the model a dependence on salinity, it was hypothesized that the relationship could be quantified by adding a salinity variable to the aggregation term of the M98 model. The results from the experiments indicate that rather than a term strictly in the aggregation term of the M98 model, salin-

ity should be included in the equation for n_f. This allows the S98 model to predict the varying growth rate observed as salinity levels change.

4.2 Final Model

Using existing experimental data [Tran et al., 2018], the W98 model was modified to include a term to limit the floc size to the Kolmogorov microscale. A series of flocculation experiments were conducted at various concentrations and salinity levels. This data was used to further modify the W98 model to create a fractal dimension equation (n_f) which is dependent on salinity. These two modifications allow for a model for floc size that is bound by the Kolmogorov microscale and that varies the growth rate with salinity. The model can be seen in equations 4.1- 4.3. This model is only currently tested for S=0-10 PSU, and is only valid for S=2.5-10 PSU; however, with more testing from salinities of S=0-2.5 PSU, and salinities greater than S=10 PSU, the model could be valid for a larger range of salinities.

$$\frac{dD}{dt} = \frac{k_A'}{n_f}\frac{{D_p}^{n_f-3}}{\rho_s}GCD^{4-n_f} - \frac{k_B'}{n_f}DG\left(\frac{D-D_p}{D_p}\right)^p\left(\frac{\mu G}{F_y/D^2}\right)^q \tag{4.1}$$

$$q = c_1 + c_2\left(\frac{D}{\eta}\right) \tag{4.2}$$

$$n_f = n_{f,0} + \frac{\log(S)S \cdot 8}{c_3} \tag{4.3}$$

While the W98 model and the M98 model are both able to capture field data fairly well, the field conditions only cover a small concentration variability with a low shear. This means that the floc size does not approach the Kologorov microscale. and thus the modified model (M98) and the original model (W98) behave similarly. When the shear is increased, as well as the concentration variability, the W98 model goes far above the expected floc size; however, the M98 model does accurately predict the floc size.

The findings from the salinity experiments were interesting as they showed something that very few studies have found before. These experiments found that a salinity increase decreased the time to equilibrium; however, it is possible that this behavior is due to a secondary repulsive force that does not adhere to the DLVO theory. Using this data it was possible to develop a model in which the growth rate varied based on salinity. This was done using a modified fractal dimension.

4.3 Future Work

The modifications to the the Winterwerp [1998] average floc size model are capable of accurately predicting floc size and floc growth while keeping floc sizes within reasonable limits and incorporating a dependence on salinity. The simplicity of these models al-

lows for them to easily be used in larger hydrodynamic and sediment transport models; However, more data is needed to better test and refine these modifications. In particular, more experiments that tease out the impact of salinity on floc size and growth rate are needed as the equation of salinity impacts was developed on a sparse set of data that did not follow conventional understanding. Additional future work would include testing the original and modified versions of the Winterwerp [1998] floc model in coupled hydrodynamic and sediment transport simulations of natural systems.

Bibliography

Physical Characteristics. https://www.chesapeakebay.net/discover/ecosystem/physical_characteristics, 2012. Accessed: 2017-03-30.

R.J. Akers, A.G. Rushton, and J.I.T. Stenhouse. Floc breakage: The dynamic response of the particle size distribution in a flocculated suspension to a step change in turbulent energy dissipation. *Chemical Engineering Science*, 42:787–798, 1987.

S Al Ani, KR Dyer, and DA Huntley. Measurement of the influence of salinity on floc density and strength. *Geo-Marine Letters*, 11(3-4):154–158, 1991.

Alice L. Alldredge and Chris Cotschalk. In situ settling behavior of marine snow. *Limnology and Oceanography*, 33(3):339–351, 1988.

Chita R. Ariathurai. *A FINITE ELEMENT MODEL FOR SEDIMENT TRANSPORT IN ESTUARIES*. PhD thesis, 1974. URL http://login.ezproxy.lib.vt.edu/login?url=https://search-proquest-com.ezproxy.lib.vt.edu/docview/302711667?accountid=14826. Copyright - Database copyright ProQuest LLC; ProQuest does not claim copyright in the individual underlying works; Last updated - 2016-05-21.

RB Biggs. Sources and distribution of suspended sediment in northern chesapeake bay. *Marine Geology*, 9(3):187–201, 1970.

DG Bowers, D McKee, CF Jago, and WAM Nimmo-Smith. The area-to-mass ratio and fractal dimension of marine flocs. *Estuarine, Coastal and Shelf Science*, 189:224–234, 2017.

K. M. Braithwaite, D. G. Bowers, W. A. M. Nimmo Smith, and G. W. Graham. Controls on floc growth in an energetic tidal channel. *Journal of Geophysical Research: Oceans*, 117 (C2), 2012.

Pierre-Yves Burban, Wilbert Lick, and James Lick. The flocculation of fine-grained sediments in estuarine waters. *Journal of Geophysical Research*, 94(C6):8323 – 8330, 1989.

Janine L Burns, Yao-de Yan, Graeme J Jameson, and Simon Biggs. A light scattering study of the fractal aggregation behavior of a model colloidal system. *Langmuir*, 13 (24):6413–6420, 1997.

T. N. Burt. Field settling velocities in estuarine muds. In Ashish J. Mehta, editor, *Estuarine Cohesive Sediment Dynamics*, pages 126–150. Springer New York, 1986.

GM Cartwright, CT Friedrichs, and LP Sanford. In situ characterization of estuarine suspended sediment in the presence of muddy flocs and pellets. *Proceedings of Coastal Sediments, Miami, FL, USA*, pages 2–6, 2011.

Shih-Nan Chen, W. Rockwell Geyer, Christopher R. Sherwood, and David K. Ralston.

Sediment transport and deposition on a river-dominated tidal flat: An idealized model study. *Journal of Geophysical Research*, 115(C10040), 2010.

Shumin Chen and Doeke Eisma. Fractal geometry of in situ flocs in the estuarine and coastal environments. *Netherlands Journal of Sea Research*, 33(2):173 – 182, 1995.

C. Coufort, D. Bouyer, and A. LinÈ. Flocculation related to local hydrodynamics in a taylor-couette reactor and in a jar. *Chemical Engineering Science*, 60(8-9):2179–2192, 2005.

B Derjaguin and L Landau. The theory of stability of highly charged lyophobic sols and coalescence of highly charged particles in electrolyte solutions. *Acta Physicochim. URSS*, 14(633-52):58, 1941.

Arne R. Diercks and Vernon L. Asper. In situ settling speed of marine snow aggregates below the mixing layer: Black Sea and Gulf of Mexico. *Deep-Sea Research I*, 44(3): 385–398, 1997.

William E. Dietrich. Settling velocity of natural particles. *Water Resources Research*, 18(6): 1615–1626, 1982.

Ian G. Droppo. Rethinking what constitutes suspended sediment. *Hydrological Processes*, 15(9):1551–1564, 2001.

K.R. Dyer. Sediment processes in estuaries: Future research requirements. *Journal of Geophysical Research*, 67(C10):14327 – 14339, 2014.

D. Eisma. Flocculation and de-flocculation of suspended matter in estuaries. *Netherlands Journal of Sea Research*, 20(2-3):183 – 199, 1986.

D. Eisma and A. Li. Changes in suspended-matter floc size during the tidal cycle in the Dollard estuary. *Netherlands Journal of Sea Research*, 31(2):107–117, 1993.

D. Eisma, P. Bernard, G.C. Cadee, V. Ittekkot, J. Kalf, R. Laane, J.M. Martin, W.G. Mook, A. van Put, and T. Schuhmacher. Suspended-matter particle size in some West-European estuaries; Part II: A review on floc formation and break-up. *Netherlands Journal of Sea Research*, 28(3):215–220, 1991.

EPA. Chesapeake bay tmdl executive summary. 2010.

M. J. Fennessy, K. R. Dyer, and D. A. Huntley. INSSEV: An instrument to measure the size and settling velocity of flocs in situ. *Marine Geology*, 117:107–117, 1994.

R.I. Ferguson and M. Church. A simple universal equation for grain settling velocity. *Journal of Sedimentary Research*, 74(6):933–937, 2004.

W. R. Geyer, P. S. Hill, and G. C. Kineke. The transport, transformation and dispersal of sediment by buoyant coastal flows. *Continental Shelf Research*, 24(7-8):927 – 949, 2004.

W Rockwell Geyer. The importance of suppression of turbulence by stratification on the estuarine turbidity maximum. *Estuaries and Coasts*, 16(1):113–125, 1993.

N. Gratiot and A.J. Manning. An experimental investigation of floc characteristics in a diffusive turbulent flow. *Journal of Coastal Research*, SI-41:105 – 113, 2004.

Chao Guo, Qing He, Leicheng Guo, and Johan C Winterwerp. A study of in-situ sediment flocculation in the turbidity maxima of the yangtze estuary. *Estuarine, Coastal and Shelf Science*, 2017.

Leicheng Guo and Qing He. Freshwater flocculation of suspended sediments in the yangtze river, china. *Ocean Dynamics*, 61:371–386, 2011.

Courtney K. Harris, Peter A. Traykovski, and W. Rockwell Geyer. Flood dispersal and deposition by near-bed gravitational sediment flows and oceanographic transport: A numerical modeling study of the Eel River shelf, northern California. *Journal of Geophysical Research*, 110(C09025), 2005.

Robert D. Hetland. The effects of mixing and spreading on density in near-field river plumes. *Dynamics of Atmospheres and Oceans*, 49(1):37 – 53, 2010.

Robert D. Hetland and Daniel G. MacDonald. Spreading in the near-field merrimack river plume. *Ocean Modelling*, 21(1–2):12 – 21, 2008.

P. S. Hill and A. R. M. Nowell. Comparison of two models of aggregation in continental-shelf bottom boundary layers. *Journal of Geophysical Research*, 100(C11):22749–22763, 1995.

Paul S. Hill, James P. Syvitski, Ellen A. Cowan, and Ross D. Powell. In situ observations of floc settling velocities. *Marine Geology*, 145:85–94, 1998.

Hening Huang. Fractal properties of flocs formed by fluid shear and differential settling. *Physics of Fluids*, 6(10):3229–3234, 1994.

K. N. Hwang. Erodibility of fine sediment in wave dominated environments. Master's thesis, University of Florida, Gainesville, FL USA, 1989.

Qing Jiang and Bruce E. Logan. Fractal dimensions of aggregates determined from steady-state size distributions. *Environmental Science & Technology*, 25(12):2031–2038, 1991.

Qing Jiang and Bruce E Logan. Fractal dimensions of aggregates from shear devices. *American Water Works Association. Journal*, 88(2):100–113, 1996.

ME Karaman, RM Pashley, TD Waite, SJ Hatch, and H Bustamante. A comparison of the interaction forces between model alumina surfaces and their colloidal properties. *Colloids and surfaces A: Physicochemical and Engineering aspects*, 129:239–255, 1997.

Ali Keyvani. *Flocculation processes in river mouth fluvial to marine transitions*. PhD thesis, University of Houston, Houston, TX, 2013.

Ali Keyvani and Kyle Strom. A fully-automated image processing technique to improve measurement of suspended particles and flocs by removing out-of-focus objects. *Computers & Geosciences*, 52:189–198, 2013.

Ali Keyvani and Kyle Strom. Influence of cycles of high and low turbulent shear on the growth rate and equilibrium size of mud flocs. *Marine Geology*, 354(0):1 – 14, 2014.

Ali Khelifa and Paul S. Hill. Kinematic assessment of floc formation using a Monte Carlo model. *Journal of Hydraulic Research*, 44(4):548–559, 2006.

C. Kranenburg. The fractal structure of cohesive sediment aggregates. *Estuarine, Coastal and Shelf Science*, 39(5):451 – 460, 1994.

R. B. Krone. Flume studies of the transport of sediment in estuarial shoaling processes. Technical report, Hydraulic Engineering Laboratory and Sanitary Engineering Research Laboratory, University of California, Berkely, CA, 1962.

R. B. Krone. Aggregation of suspended particles in estuaries. In B. Kjerfve, editor, *Estuarine transport processes*, pages 177–190. University of South Carolina Press, 1978.

Ray B Krone. A study of rheologic properties of estuarial sediments. Technical report, CALIFORNIA UNIV BERKELEY SANITARY ENGINEERING RESEARCH LAB, 1963.

Ray B. Krone. *The Significance of Aggregate Properties to Transport Processes*, pages 66–84. Springer New York, New York, NY, 1986. ISBN 978-1-4612-4936-8. doi: 10.1007/978-1-4612-4936-8_4. URL http://dx.doi.org/10.1007/978-1-4612-4936-8_4.

Remya G. Kumar, Kyle B. Strom, and Ali Keyvani. A lattice boltzmann model for the non-equilibrium flocculation of cohesive sediments in turbulent flow. *Continental Shelf Research*, 30(20):2067 – 2081, 2010.

G. F. Lane-Serff. Investigation of the fractal structure of jets and plumes. *Journal of Fluid Mechanics*, 249:521–534, 1993.

Byung Joon Lee, Erik Toorman, Fred J. Molz, and Jian Wang. A two-class population balance equation yielding bimodal flocculation of marine or estuarine sediments. *Water Research*, 45(5):2131 – 2145, 2011.

Du Gon Lee, James S Bonner, Laurie S Garton, Andrew NS Ernest, and Robin L Autenrieth. Modeling coagulation kinetics incorporating fractal theories: comparison with observed data. *Water Research*, 36(4):1056–1066, 2002.

V. G. Levich. *Physicochemical Hydrodynamics*. Prentice Hall, 1962.

Dongyi Li, Yunhai Li, and Yonghang Xu. Observations of distribution and flocculation of suspended particulate matter in the minjiang river estuary, china. *Marine Geology*, 2017.

Wilbert Lick and James Lick. Aggregation and disaggregation of fine-grained lake sediments. *Journal of Great Lakes Research*, 14(4):514 – 523, 1988.

Bruce E. Logan. *Environmental Transport Processes*. John Wiley & Sons, 1999.

Bruce E Logan. *Environmental transport processes*. John Wiley & Sons, 2012.

Joeran Maerz and Kai Wirtz. Resolving physically and biologically driven suspended particulate matter dynamics in a tidal basin with a distribution-based model. *Estuarine, Coastal and Shelf Science*, 84(1):128 – 138, 2009.

Joeran Maerz, Romaric Verney, Kai Wirtz, and Ulrike Feudel. Modeling flocculation pro-

cesses: Intercomparison of a size class-based model and a distribution-based model. *Continental Shelf Research*, 31(10, Supplement):S84 – S93, 2011.

A.J. Manning and K.R. Dyer. A laboratory examination of floc characteristics with regard to turbulent shearing. *Marine Geology*, 160(1-2):147 – 170, 1999.

Thor Nygaard Markussen and Thorbjørn Joest Andersen. Flocculation and floc break-up related to tidally induced turbulent shear in a low-turbidity, microtidal estuary. *Journal of sea research*, 89:1–11, 2014.

W.H. McAnally and A.J. Mehta. Collisional aggregation of fine estuarial sediment. In William H. McAnally and Ashish J. Mehta, editors, *Coastal and Estuarine Fine Sediment Processes*, volume 3 of *Proceedings in Marine Science*, pages 19 – 39. Elsevier, 2000a.

William H. McAnally and Ashish J. Mehta. Aggregation rate of fine sediment. *Journal of Hydraulic Engineering*, 126(12):883–892, 2000b.

I.N. McCave. Size spectra and aggregation of suspended particles in the deep ocean. *Deep Sea Research*, 31(4):107 – 122, 1984.

Francesca Mietta. *Evolution of the floc size distribution of cohesive sediments*. PhD thesis, Delft University of Technology, Delft, the Netherlands, 2010.

C Migniot. A study of the physical properties of various forms of very fine sediments and their behavior under hydrodynamic actions. *La Houille Blanche*, (7), 1968.

Daniel Mikeš and Andrew James Manning. Assessment of flocculation kinetics of cohesive sediments from the Seine and Gironde estuaries, France, through laboratory and field studies. *Journal of Waterway, Port, Coastal, and Ocean Engineering*, 136(6):306–318, 2010.

T.G. Milligan and P.S. Hill. A laboratory assessment of the relative importance of turbulence, particle composition, and concentration in limiting maximal floc size and settling behaviour. *Journal of Sea Research*, 39(3–4):227 – 241, 1998.

I. Nezu and H. Nakagawa. *Turbulence in open-channel flows*. A. A. Balkema, Rotterdam, 1993.

V. Oles. Shear-induced aggregation and breakup of polystyrene latex-particles. *Journal of Colloid and Interface Science*, 154(2):351–358, 1992.

MW Owen. *A detailed study of the settling velocities of an estuary mud*. Hydraulics Research Station, 1970.

MW Owen. The effect of turbulence on the settling velocities of silt flocs. In *Proceedings of the Fourteenth Congress of IAHR*, volume 4, pages 27–32, 1971.

D. Parker, W. J. Kaufman, and D. Jenkins. Floc breakup in turbulent flocculation processes. *Journal of the Sanitary Engineering Division, ASCE*, 98(SA1):79–97s, 1972.

Eric N Partch and J Dungan Smith. Time dependent mixing in a salt wedge estuary. *Estuarine and Coastal Marine Science*, 6(1):3–19, 1978.

Emmanuel Partheniades. *Cohesive Sediments in Open Channels*. Butterworth-Heinemann/Elsevier, Burlington, MA, 2009.

Luís Ivens Portela, Susana Ramos, and António Trigo Teixeira. Effect of salinity on the settling velocity of fine sediments of a harbour basin. *Journal of Coastal Research*, 65 (sp2):1188–1193, 2013.

Rafael Ramírez-Mendoza, Alejandro J Souza, Laurent O Amoudry, and Andrew J Plater. Effective energy controls on flocculation under various wave-current regimes. *Marine Geology*, 382:136–150, 2016.

W. W. Rubey. Settling velocity of gravel, sand, and silt particles. *American Journal of Science*, 25(148):325–338, 1933.

Lawrence P Sanford, Steven E Suttles, and Jeffrey P Halka. Reconsidering the physics of the chesapeake bay estuarine turbidity maximum. *Estuaries and Coasts*, 24(5):655–669, 2001.

C Schwarz, T Cox, T Van Engeland, D van Oevelen, J van Belzen, J van de Koppel, K Soetaert, Tjeerd J Bouma, P Meire, and S Temmerman. Field estimates of floc dynamics and settling velocities in a tidal creek with significant along-channel gradients in velocity and spm. *Estuarine, Coastal and Shelf Science*, 197:221–235, 2017.

Malcolm E Scully and Carl T Friedrichs. Sediment pumping by tidal asymmetry in a partially mixed estuary. *Journal of Geophysical Research: Oceans*, 112(C7), 2007.

Ashoke K. SenGupta and Kyriakos D. Papadopoulos. Stability of concentrated colloids: The controlling parameters. *Journal of Colloid and Interface Science*, 203:345–353, 1998.

Teresa Serra, Jordi Colomer, and Xavier Casamitjana. Aggregation and breakup of particles in a shear flow. *Journal of COlloid and Interface Science*, 187(CS964710):87 – 95, 1996.

Teresa Serra, Jordi Colomer, and Bruce E. Logan. Efficiency of different shear devices on flocculation. *Water Research*, 42:1113–1121, 2008.

Xiaoteng Shen and Jerome P.-Y. Maa. Modeling floc size distribution of suspended cohesive sediments using quadrature method of moments. *Marine Geology*, 359:106 – 119, 2015. ISSN 0025-3227.

C. R. Sherwood, A. L. Aretxabaleta, C. K. Harris, J. P. Rinehimer, R. Verney, and B. Ferre. Cohesive and mixed sediment in the regional ocean modeling system (roms v3.6) implemented in the coupled ocean atmosphere wave sediment-transport modeling system (coawst r1179). *Geoscientific Model Development Discussions*, 2017:1–43, 2017.

M. Son and T.-J. Hsu. The effect of variable yield strength and variable fractal dimension on flocculation of cohesive sediment. *Water Research*, 43(14):35823592, 2009.

Minwoo Son and Tian-Jian Hsu. Flocculation model of cohesive sediment using variable fractal dimension. *Environmental Fluid Mechanics*, 8(1):55–71, 2008.

R. W. Sternberg, A. Ogston, and R. Johnson. A video system for in situ measurement

of size and settling velocity of suspended particulates. *Journal of Sea Research*, 36(1/2): 127–130, 1996.

K. D. Stolzenback and M. Elimelich. The effect of density on collisions between sinking particles: implications for particle aggregation in the ocean. *Journal of Deep Sea Research I*, 41(3):469–483, 1994.

M Stone and BG Krishnappan. Floc morphology and size distributions of cohesive sediment in steady-state flow. *Water Research*, 37(11):2739–2747, 2003.

Kyle Strom and Ali Keyvani. An explicit full-range settling velocity equation for mud flocs. *Journal of Sedimentary Research*, 81(12):921–934, 2011.

Kyle Strom and Ali Keyvani. Flocculation in a decaying shear field and its implications for mud removal in near-field river mouth discharges. *Journal of Geographic Research*, 121:21422162, 2016.

James P. M. Syvitski, K. W. Asprey, and K. W. Leblanc. In-situ characteristics of particles settling within a deep-water estuary. *Deep-Sea Research II*, 42(1):223–256, 1995.

Norihito Tambo and Hitoshi Hozumi. Physical aspects of flocculation process–II. contact flocculation. *Water Research*, 13:441–448, 1979.

Fiona H.M. Tang, Fernando Alonso-Marroquin, and Federico Maggi. Stochastic collision and aggregation analysis of kaolinite in water through experiments and the spheropolygon theory. *Water Research*, 53:180 – 190, 2014.

Santosh L Tawari, Donald L Koch, and Claude Cohen. Electrical double-layer effects on the brownian diffusivity and aggregation rate of laponite clay particles. *Journal of Colloid and Interface Science*, 240(1):54–66, 2001.

H. Tennekes and J. L. Lumley. *A First Course in Turbulence*. MIT Press, 1972.

Duc Tran, Rachel Kuprenas, and Kyle Strom. How does sediment concentration influence the growth rate and equilibrium size of mud flocs under steady turbulent shearing? *in review with Continental Shelf Research*, 2018.

Cheng-Han Tsai, Sam Iacobellis, and Wilbert Lick. Flocculation of fine-grained lake sediments due to a uniform shear stress. *Journal of Great Lakes Research*, 13(2):135–146, 1987.

W. van Leussen. Aggregation of particles, settling velocity of mud flocs: a review. In J. Dronkers and W. van Leussen, editors, *Physical processes in estuaries*, pages 347–403. Springer- Verlag, Berlin, 1988.

W. Van Leussen. *Estuarine macroflocs and their role in fine-grained sediment transport*. PhD thesis, University of Utrecht, Utrecht, The Netherlands, 1994.

Wim van Leussen. The variability of settling velocities of suspended fine-grained sediment in the Ems estuary. *Journal of Sea Research*, 41:109–118, 1999.

Romaric Verney, Robert Lafite, and Jean-Claude Brun-Cottan. Flocculation potential of estuarine particles: The importance of environmental factors and of the spatial and

seasonal variability of suspended particulate matter. *Estuaries and Coasts*, 32(4):678–693, 2009.

Romaric Verney, Robert Lafite, Jean Claude Brun-Cottan, and Pierre Le Hir. Behaviour of a floc population during a tidal cycle: Laboratory experiments and numerical modelling. *Continental Shelf Research*, 31(10):S64–S83, 2011.

EJ Verwey and J Th Overbeek. Theory of the stability of colloidal dispersions, 1948.

TD Waite, JK Cleaver, and JK Beattie. Aggregation kinetics and fractal structure of γ-alumina assemblages. *Journal of Colloid and Interface science*, 241(2):333–339, 2001.

Mark R. Wiesner. Kinetics of aggregate formation in rapid mix. *Water Research*, 26(3):379 – 387, 1992.

Johan C. Winterwerp. A simple model for turbulence induced flocculation of cohesive sediment. *Journal of Hydraulic Research*, 36(3):309–326, 1998.

Johan C. Winterwerp. On the flocculation and settling velocity of estuarine mud. *Continental Shelf Research*, 22:1339–1360, 2002.

Johan C. Winterwerp and Walther G. M. van Kesteren. *Introduction to the physics of cohesive sediment in the marine environment*, volume 56 of *Developments in Sedimentology*. Elsevier, Amsterdam, The Netherlands, 2004.

X. M. Xia, Y. Li, H. Yang, C. Y. Wu, T. H. Sing, and H. K. Pong. Observations on the size

and settling velocity distributions of suspended sediment in the Pearl River Estuary, China. *Continental Shelf Research*, 24(16):1809–1826, 2004.

Fanghua Xu, Dong-Ping Wang, and Nicole Riemer. An idealized model study of flocculation on sediment trapping in an estuarine turbidity maximum. *Continental Shelf Research*, 30(12):1314–1323, 2010.